POLITECNICO DI MILANO

Dipartimento di Ingegneria Civile e Ambientale

Corso di Laurea Magistrale in Ingegneria per l'Ambiente e il Territorio

ANALYSIS OF ENHANCED PRESSURIZED WEATHERING OF LIMESTONE AS A TECHNOLOGY FOR CO_2 STORAGE

Relatore: Prof. Stefano Caserini

Correlatore: Ing. Giovanni Cappello

Elaborato di laurea di:

Davide Righi

Matr. 898378

Anno accademico 2019/2020

Ringraziamenti

Ringrazio il professor Stefano Caserini per la disponibilità, la competenza, il supporto ed il tempo che mi ha dedicato, al fine di permettermi di portare a termine il presente elaborato.

Ringrazio l'ingegnere Giovanni Cappello per la grande disponibilità e competenza con cui mi ha seguito durante lo svolgimento di questo lavoro.

Ringrazio la mia famiglia che mi ha sempre supportato e ha sempre creduto in me, permettendomi di scegliere il percorso migliore per me.

Ringrazio infine tutti gli amici che mi hanno accompagnato in questo percorso, facendo letteralmente volare questi anni.

Table of Contents

List of Figures

List of Tables

Chapter 1: INTRODUCTION

Carbon dioxide (CO_2) is the principal anthropogenic contributor to the greenhouse effect, and then it plays a significant role in global warming. The burning of fossil fuels and other anthropogenic activity has dramatically increased the concentration of atmospheric CO_2 compared to its value over the previous 800,000 years (IPCC, 2013). The reduction of this concentration is then considered as a first step to reduce climate change.

The continuous addition of CO_2 to the atmosphere has changed the natural equilibrium of carbon that had been in equilibrium for the previous 10,000 years. In particular, the perturbation started with the first industrial revolution due to fossil fuels' use. This has caused an increase in the global temperature compared to the pre-industrial level (IPCC, 2013).

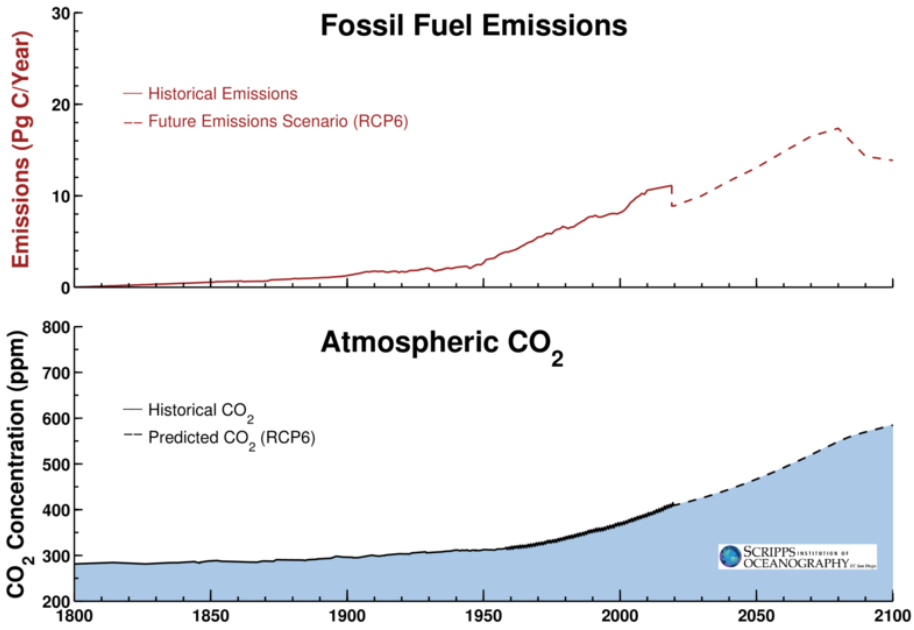

Figure 1-1: CO_2 concentrations in atmosphere and fossil fuel emissions from 1800 to 2100 Scripps Institution of Oceanography, 2020)

The massive use of fossil fuels has increased the concentration of CO_2 in the atmosphere, as shown in Figure 1-1, and right now, atmospheric CO_2 concentration is 411 ppm (Scripps Institution of Oceanography, 31 August 2020). Hansen et al. (2008) proposed a "safety level" for the concentration of CO_2 in the atmosphere in the long term at about 350 ppm. This value derives from the analysis of past modifications of the climate system that caused

essential impacts. Since the concentration of CO_2 is already higher than this “safety level”, reaching this value is necessary not only to stop the emission of carbon dioxide in the atmosphere but also to absorb a part of it through a portfolio of methods called "negative emission".
The globally averaged combined land and ocean surface temperature data as calculated by a linear trend, show a warming of 0.85 [0.65 to 1.06] °C, over the period 1880-2012, when multiple independently produced dataset exist. The total increase between the average of the 1850-1900 period and the 2003-2012 periods is 0.78 [0.72 to 0.85] °C based on the single longest dataset available (IPCC, 2013).
Based on climate model studies and the Earth's history, additional global warming of about 1°C or more, above the global temperature in 2000, is likely to be dangerous (Hansen, 2008).

The multilateral effort of limiting global warming is mainly structured in the international climate negotiations, that started with the UNFCCC, United Nations Framework Convention on Climate Change, signed in Rio de Janeiro in 1992. In this framework, the ambitious objective is to avoid any dangerous anthropogenic interference on the climate system. 26 conferences of the parties and protocols have been done through the years, and the last one of these is the Paris Agreement, signed in 2015.
The objective of the Paris Agreement is ambitious, limit global warming well below 2 °C, with respect to the pre-industrial levels, and make efforts to limit the increase of temperature below 1.5 °C, and this requires a rapid decrease in GHG emissions and then the removal of large quantities of CO_2 from the atmosphere (IPCC, 2013).

Various methods have been proposed to mitigate anthropogenic CO_2 released into the atmosphere. In this study, the focus will be on Carbon Capture and Storage (CCS) technologies that consist of the separation of CO_2 from flue gas produced in power stations or other industrial sources and its subsequent underground storage. Several capture technologies are already at a commercial level, while on the storage phase, that will be the focus of this thesis, the different methods are at low levels of development.
In Chapters 2 and 3, a bibliographic review of the different CO_2 storage technologies has been carried out to evaluate their current development and assess the various strengths and weaknesses.

Among storage technologies, the geological storage of CO_2 in saline formations is the most advanced technology. Still, it has some drawbacks, like the costs and the energy required to bring CO_2 to the supercritical state. Furthermore, to avoid the possibility of leakage and its disastrous consequences, it is necessary to evaluate the cap rock's stability, i.e., the impermeable layer under which the carbon dioxide is stored. For these reasons, it is important to define alternative ways to sequester CO_2 both considering underground storage (carbonate water injection) and ocean storage, such as confined submarine carbon storage in glass capsules (Caserini et al., 2017) and enhanced weathering of limestone (Rau and Caldeira, 1999, 2000), that consists in the reaction of CO_2 from power plant waste gas with seawater and carbonate minerals ($CaCO_3$), calcite or aragonite, with a final discharge into the ocean.

After this review, the study will focus on the Enhanced Pressurized Weathering of Limestone (EPWL) storage method, proposed by Cappello and Ross Morrey. This technology is an evolution of the Enhanced Weathering of Limestone (EWL). It is studied in detail in chapters 4 and 5, assessing the feasibility and amounts of seawater and carbonate minerals needed to dissolve CO_2.

Two different configurations are considered, depending on the depth of the sea at a particular location. Suppose the solution is discharged below 5,000 m, i.e., the Carbonate Compensation Depth (CCD). In that case, the solution can be released even if the dissolution of carbonate minerals has not been completed yet, since below CCD no calcite is preserved in seawater after discharge. This method is called Enhanced Pressurized Weathering of Limestone (EPWL) in this study.

In places with lower sea depth, like the Mediterranean Sea, where the CCD is never reached, the EPWL method could not be applied because there is the need to dissolve all the carbonate minerals before the end of the pipe, since the release of unreacted minerals above the CCD results in their precipitation, and the EPWL configuration requires too much water. A new configuration has then been studied to overcome the problem of using a large amount of water to discharge an ionic solution into the sea between the Aragonite Compensation Depth (ACD) and the CCD, the pH Adjusted –Enhanced Pressurized Weathering of Limestone (pHA-EPWL): it adds to EPWL a floating reactor where a final carbonate mineral dissolution and pH adjustment is realized using a natural confined flow of seawater at first and secondly by the addition of calcium hydroxide. The latter buffers the remaining CO_2 to increase the pH of the final discharge in the open waters and to guarantee complete CO_2 storage in the bicarbonate form.

In chapter 6, two study cases for the technologies are presented, assessing the amounts of reactants needed, the pipes' size, and preliminary cost evaluations.

Chapter 2: TRADITIONAL GEOLOGICAL STORAGE

2.1 Current status of Carbon Capture and Storage development

Carbon Capture and Storage (CCS) consists in the separation of CO_2 from flue gas produced in power stations or other industrial sources and its subsequent underground storage.
The most used capture technology is after combustion through chemical absorption, using aqueous amine solutions. Before the storage, the CO_2 is transported from source to storage, and this is made through pipelines, both on-shore and off-shore, or ships.
There is a suite of technologies being developed for the capture, transport, and storage of CO_2. In Figure 2-1 are summarized the current development progress of different CCS methods on the basis of their Technology readiness levels (TRL). TRL is a method for measuring the maturity of technologies during the development phase of them. They are based on a scale from 1 to 9, with 9 for the most mature technology.

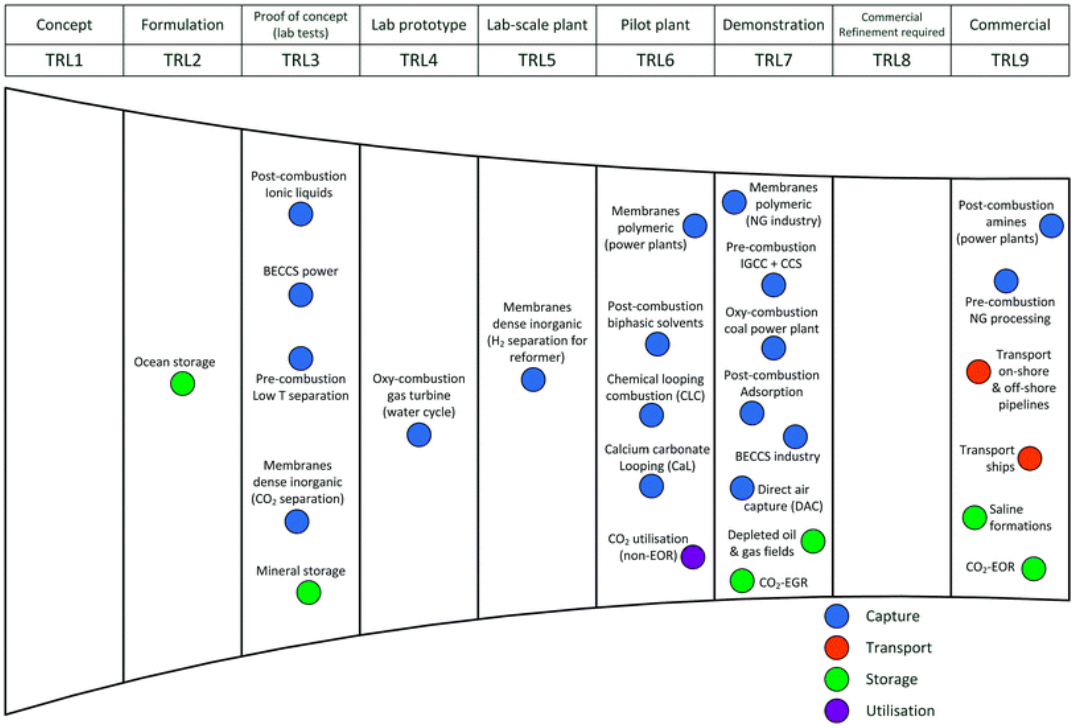

Figure 2-1: Current development of carbon capture, storage, and utilization technologies in terms of Technology Readiness Levels (Bui et al., 2018)

Figure 2-1 shows that various technologies for CO_2 capture are at high development stages and that the transport technologies are at the commercial level, i.e., fully operational. This study will focus on the different technologies for CO_2 storage that are at a minor development stage.

CCS has the potential to provide emissions cuts sufficient to stabilize greenhouse-gas concentrations in the atmosphere while still allowing them to continue to use fossil fuels. This method can act as a transitional technology to buy time to improve renewable energy generation (Bui et al., 2018).

One of the critical attributes of this sequestration method is that it can be applied to many carbon-emitting sectors and is ideal for system-wide decarbonization efforts (Bui et al., 2018).

An important focus will need to be on the development of CCS infrastructure to which multiple CO_2 sources can connect to take advantage of economies of scale and to optimize the development pathway, following the Sleipner example in the North Sea (Torp and Gale, 2004).

The problem is that the need for CCS has not been framed so that it is attractive or rationale for the private sector to finance CCS projects. The physical and economic risks associated with the development of large scale CCS projects and the associated CO_2 transport and storage infrastructure have so far outweighed the potential rewards on offer, as evidenced by the abandonment of many tens of promising projects around the world (Bui et al., 2018).

The value of CCS derives from the fact that it is the only technology that can simultaneously address carbon reduction objectives across many carbon-emitting sectors of the economy without compromising their cost-effective service provision. However, it has barely reached the levels indicated by the projection of the International Energy Agency (IEA) because of the opposition of many governments, which are motivated by perceived uncertainties concerning its safety and the fear that it will serve to extend the dependence on fossil fuels and be a barrier to greater utilisation of renewable power (Bui et al., 2018).

2.2 Regional analysis

In 2019 the number of large scale CCS facilities increased to 51, of which:

- 19 are operating
- 4 are under construction
- 10 are in advanced development
- 18 are in early development.

The location of these facilities is shown in Figure 2-2.

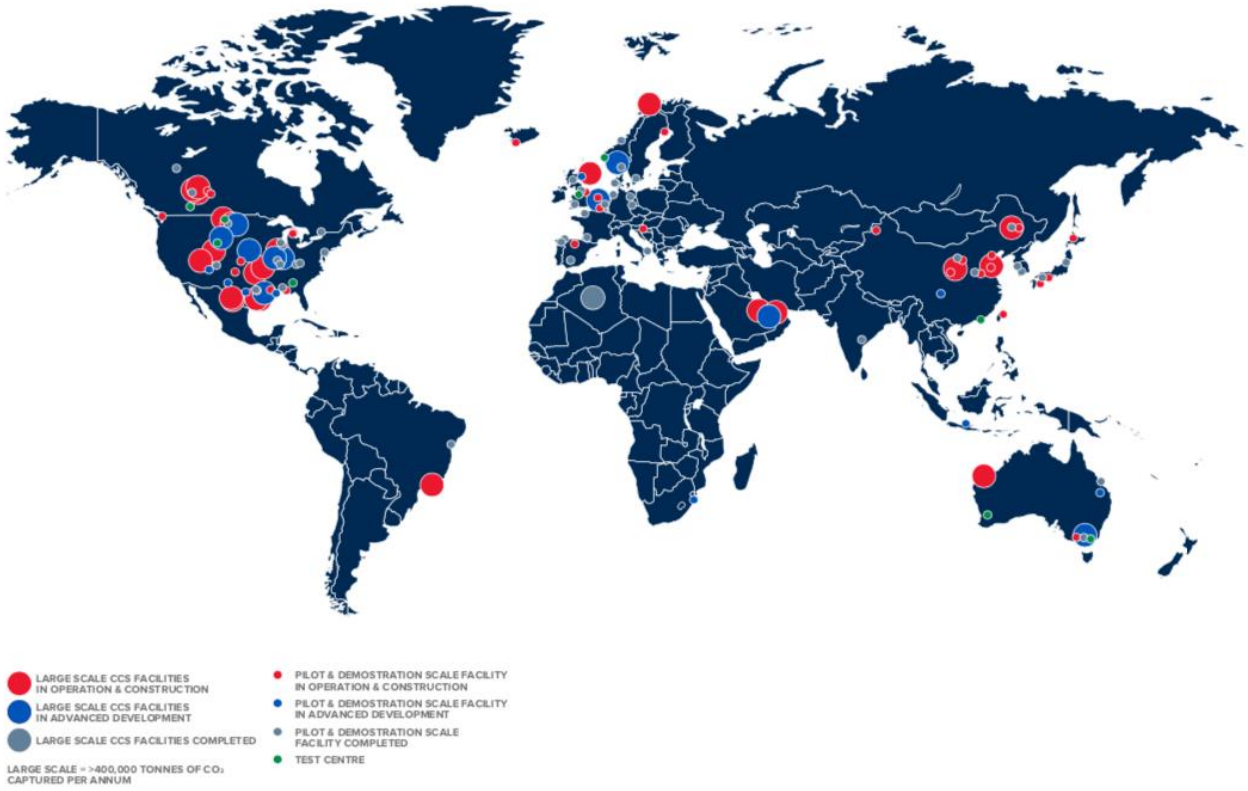

Figure 2-2: CCS facilities around the world in 2019 (Global CCS Institute, 2019)

Those in operation and construction can capture and permanently store around 40 million tonnes of CO_2 every year. This is expected to increase by about one million tonnes in the next 12-18 months from 2019. Also, there are 39 pilot demonstration-scale CCS facilities (operating or about to commissioned) and nine CCS technology test centers (Global CCS Institute, 2019).

The Americas, considering Canada, United States, Central, and South America, store 29.9 Million tonnes per annum (Mtpa) of CO_2 since they are home to 13 of the world's large-scale operating CCS facilities.

In Europe, there are 2 large scale CCS facilities in operation in Norway, capturing and storing 1.7 Mtpa of CO_2, and there are 10 large scale facilities that, when operational, will capture 20.8 Mtpa of CO_2.

In the Middle East and Central Asia, 2 large scale CCS facilities are in operation, capturing 1.6 Mtpa of CO_2. This region has a vast and accessible underground storage potential of 5-30 Gigatonnes.

The Asia Pacific, a region that comprehends China, India, Japan, and Australia, is the source of just over 50% of the world's total CO_2 emission, which is driven by fossil fuel reliance. This region has 12 large-scale facilities, either operating or in various stages of development.

The CCS facilities can store a massive amount of CO_2, but currently, only 0.1% of the global emissions are safely stored by these technologies.

2.3 Geological storage

The most advanced technology to store CO_2 is geological storage. It has a TRL level of 9, and all the operating large-scale CCS facilities use this technology, so it stores about 33.2 $MtCO_2$/year around the world, 40 $MtCO_2$/year also considering the facilities in construction (Global CCS Institute, 2019).

The CO_2 is generally injected underground as a so-called supercritical fluid. In this state, the CO_2 has a liquid-like density and flows like a gas, and with a decrease in pressure, it will expand to form a gas without a phase transition, i.e., it will not boil. The CO_2 density will still be less than the surrounding water. The viscosity is typically less than a tenth of the rock's brine resident (Blunt, 2010). The injected CO_2 will migrate to the top of the rock layer because of buoyancy forces.

There are four principal ways in which the CO_2 is prevented from reaching the surface:

- Structural or stratigraphic trapping refers to low-permeability layers of rock (the so-called cap rock) that prevent the upwards movement of CO_2.
- Dissolution of CO_2 in the formation brine forming a denser phase that will sink.
- The CO_2 dissolved in brine forms a weakly acidic solution that may react over thousands to millions of years with the host rock, forming solid carbonate.
- Capillarity trapping occurs when water displaces CO_2 in the pore space. Water tends to wet the surface, leaving the CO_2 surrounded by water in pore-space bubbles that cannot escape.

The supercritical CO_2 has the density of water but the gas's viscosity, so it penetrates easily. It is lighter, so it goes to position itself next to the cap rock. This requires that the cap rock has to be intact, so preliminary assessments have to be done.

Geological sinks for CO_2 include deep saline formations, depleted oil and gas reservoirs, and unmineable coal seams. These formations are widely dispersed around the world and together can hold the storage of hundreds to thousands of GtC. Oil and gas reservoirs are a good option because of their ability to contain pressurized fluids for long periods. If CO_2 is injected into active oil reservoirs, the added economic benefit earning from Enhanced Oil Recovery (EOR) could offset some of the sequestration costs (Herzog and Vukmirovic, 2000).

Deep saline formations (>800 m) may be the best-long term geologic storage option because their potential storage is extensive and widely distributed. These solutions should be located under a relatively impermeable cap, yet there should be high permeability and porosity below the cap rock to allow the CO_2 to be distributed efficiently. (Herzog and Vukmirovic, 2000).

Abandoned and uneconomic coal seams are another potential storage site. CO_2 diffuses through the coal's pore structure, and then it is physically absorbed into the coal. CO_2 can also be used to enhance the recovery of coal bed methane.

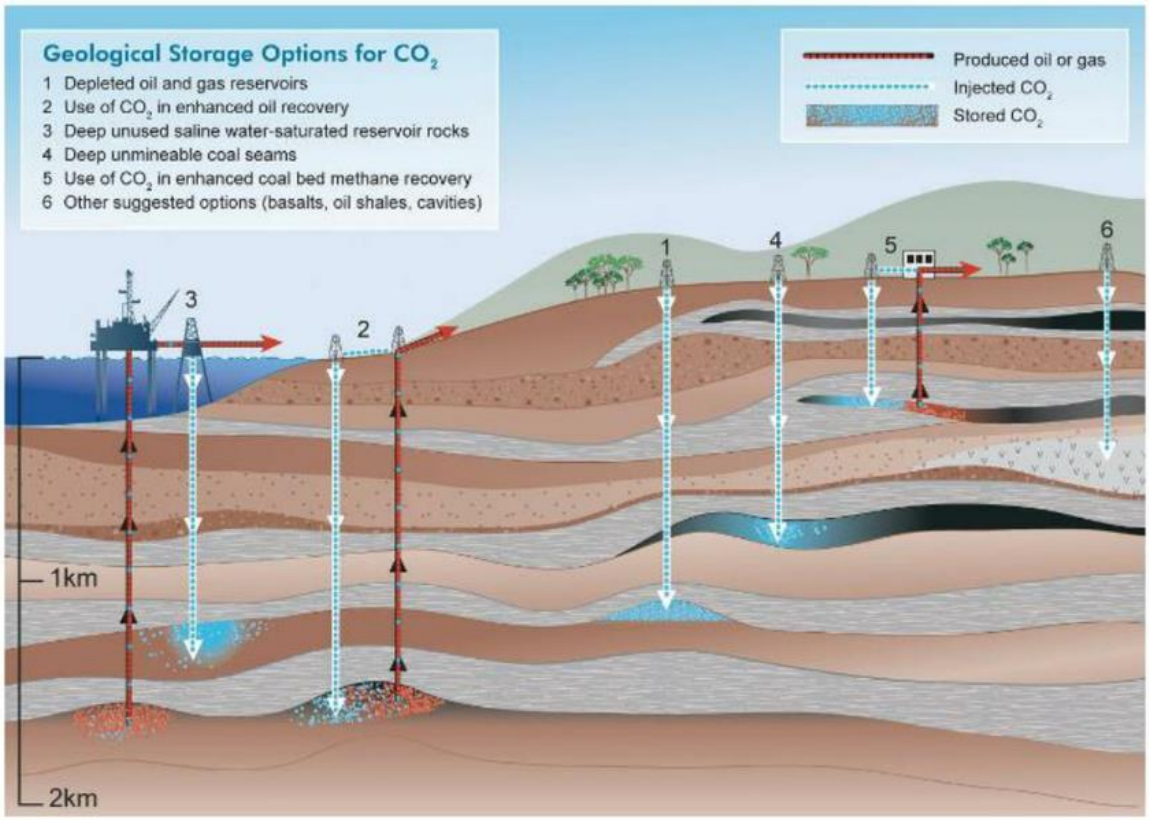

Figure 2-3: Geological storage options for CO_2 (Strogen et al., 2009)

The costs for geological storage are typically between 0.5-8 $/t$CO_2$ stored (IPCC, 2013). The full range of cost estimates for individual options is huge. Cost information for the quality of the cap rock and storage monitoring has to be added. When storage is combined with EOR, enhanced oil recovery, enhanced production benefits can offset some of the capture and storage costs.

There are some risks related to geological storage. The primary and most important risk factor is leakage that could be as a result of:

- aquifer over-pressurization that could lead to cracks in the cap rock overlying it and in the reactivation of faults.
- Abandoned wells, they are more plausible in depleted hydrocarbon reservoir which has been used previously for the commercial production of hydrocarbon dioxides than in saline aquifers. This is because depleted hydrocarbon dioxide reservoirs possess wells whose structural integrity might have degraded over time.
- Faults and fractures, it is essential to ensure that there are no transmissive faults and fractures in the identified formation. Additionally, during the injection of CO_2,

care must be taken to ensure that inactive faults are not activated due to the high aquifer pressures (Ajayi et al., 2019).

Another risk associated with CO_2 storage is induced seismicity. This could lead to earthquakes that exceed magnitudes of M6 and have the potential to impact the containment, infrastructure, and public perceptions of safety at CO_2 storage sites. The possibility of a seismic event will be higher if faults are present (Ajayi et al., 2019).

This process also requires a lot of time and investments for the geological analysis of the presence and the integrity of the cap rock. The initial costs of drilling and installation are high. Also, there are the monitoring costs, since the integrity of the cap rock has to be assured and the integrity of the pipe that needs to be secured.

Chapter 3: ALTERNATIVE CO_2 STORAGE METHODS

In this third chapter, this study will focus on the following CO_2 storage options:

- Carbonated Water Injection
- Direct ocean storage
- Confined Submarine Carbon Storage
- Enhanced Weathering of Limestone

3.1 Carbonated Water Injection

An alternative CO_2 injection strategy is Carbonated Water Injection (CWI) that consists of the injection of water saturated with CO_2 in saline aquifers. In carbonated water, CO_2 exists as a dissolved phase instead of a free phase eliminating the problems of gravity segregation and low sweep efficiency, characteristics of a typical CO_2 injection project. Indeed, both viscosity and density of water increase due to the dissolution of CO_2 in water. This process can be done with brine waters from deep saline aquifers. Brine waters are water with a high concentration of sodium chloride.

CO_2 solubility in brine, at constant temperature and salinity, increases with increasing pressure. With increasing temperature, the solubility of CO_2 decreases even at increasing pressure. Thus, the best conditions for having a more significant dissolution of CO_2 in brine are higher pressure and lower temperature (Shariatipour et al., 2016). For this reason, a feasible solution would be to use brine from deep aquifers for the scrubbing because it is already at high pressure, and when it mixes with the CO_2, it greatly increases the solubility and reduces the volume of brine required.

A surface-dissolution approach involves dissolving captured dense CO_2 into the brine in surface facilities, and the CO_2-saturated brine is then injected into the storage formation. The brine required for the CO_2 surface mixing is extracted from the same formation used for storage (Eke et al., 2011). The injection point is around 700 m depth.

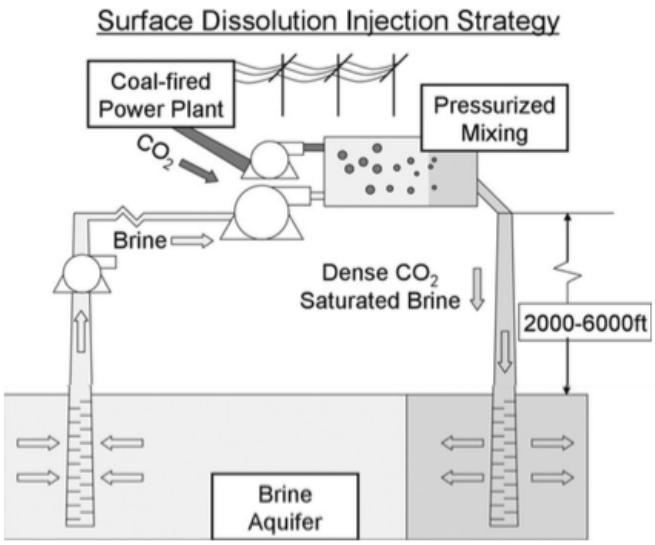

Figure 3-1: Schematic of the brine-dissolution strategy (Burton and Bryant, 2009)

If the gas is scrubbed with brine, there is no need for the cap rock, since the input liquid is heavier and goes to the bottom of the aquifer. It is also absent the need to evaluate the cap rock's integrity, so the overall costs are reduced.

The denser CO_2-saturated-brine stream, when injected into the formation, is able to eliminate the buoyancy force that is a strong driving force to bring CO_2 to the surface. (Eke et al., 2011). Storing CO_2 in dissolved form avoids the formation of a gas bubble in the aquifer and, therefore, the associated risks of buoyancy, causing the gas to rise and leak to the surface. The chance of the injected CO_2 escape to the surface is thus low-to-inexistent as it remains trapped by dissolution in the brine. There is no pressure build-up in the aquifer because the amount of pumped water exactly balances the amount of injected water. Also, experiments show that CWI, compared to pure water injection, improves oil recovery as both secondary (before water flooding) and tertiary (after water flooding) recovery methods. The dissolved carbon dioxide will transfer from the water phase to the oil phase due to the potential chemical difference of the CO_2 in two steps (as a driving force). This interphase mass transfer reduces the oil viscosity, lowers the oil-water interfacial tension, and causes oil swelling, which will be responsible for the reconnection of isolated residual oil, mobilizing the trapped oil (after CWI) to be produced. These mechanisms will result in a higher oil recovery factor upon CWI (Esene et al., 2018).

This method's problem is that the interaction between the injected carbonated water and reservoir rock can lead to various chemical reactions, especially in carbonates. The

reaction will influence the fluid-flow and oil recovery mechanisms of reactive transport in porous media. Upon the reactions, the reservoir's mechanical properties will be affected, resulting in the loss of reservoir formation integrity.
It is challenging to prepare the CW at large scales and under desired pressure and temperature conditions. Another issue is the corrosion of the process facilities due to the formation of carbonic acid due to CO_2 dissolution in water.
The CWI could also create water weakening effects, so the deformation of reservoir layers. This causes several issues, including reservoir compaction and seabed subsidence.

There are already some field experiments using this technology, so it has a TRL of 5-6. The overall cost considering gas mixture capture, transport, and storage is about 21.3 $/t$CO_2$ stored (Gunnarsson et al., 2018).

An important CWI plant is called CarbFix and is located in Hellisheidi, Iceland. This injection site is situated about 3 km south of the Hellisheidi geothermal powerplant. This plant requires 25 tonnes of water per tonne of CO_2 stored (Matter et al., 2016).
Matter et al. (2016) demonstrate that over 95% of the CO_2 injected into the CarbFix site in Iceland was mineralized to carbonate minerals in less than 2 years.

3.2 Direct ocean storage

The ocean has a large uptake capacity. It currently contains an estimated 40,000 Gt C (billion tonnes of carbon), mostly in dissolved organic ions. This compares with about 800 Gt C in the atmosphere and 2,000 Gt C in the land biosphere. Thus, the amount of carbon that would cause a doubling of the atmospheric concentration would only change the ocean concentration by about 2 % (Adams and Caldeira, 2008).
The CO_2 is already indirectly discharged into the surface ocean when it is emitted to the atmosphere. Because fossil carbon emissions are large, the atmosphere and the ocean are currently out of chemical equilibrium, causing a net flux of about 8 Gt CO_2 per year (2 Gt C per year). Over a period of centuries, 70-80% of present day-emissions will ultimately reside in the ocean. Discharging CO_2 directly into the deep sea would accelerate this natural process, thus reducing peak atmospheric concentrations and protecting ocean surface waters with a slower rate of CO_2 increase (Adams and Caldeira, 2008).

Various methods to store CO_2 in the ocean have been proposed (IEA Greenhouse Gas R&D Programme, 2010), including:

- CO_2 dispersal in a very dilute form at depths of 1,000-2,000 m.
- Discharge at 3,000 m to form a lake of liquid CO_2 on the seabed.
- Formation of a sinking plume to carry most of the CO_2 into deeper water.
- Release of solid CO_2 at depth in the form of hydrate.

Different options for ocean storage of CO_2 are also shown in Figure 3-2.

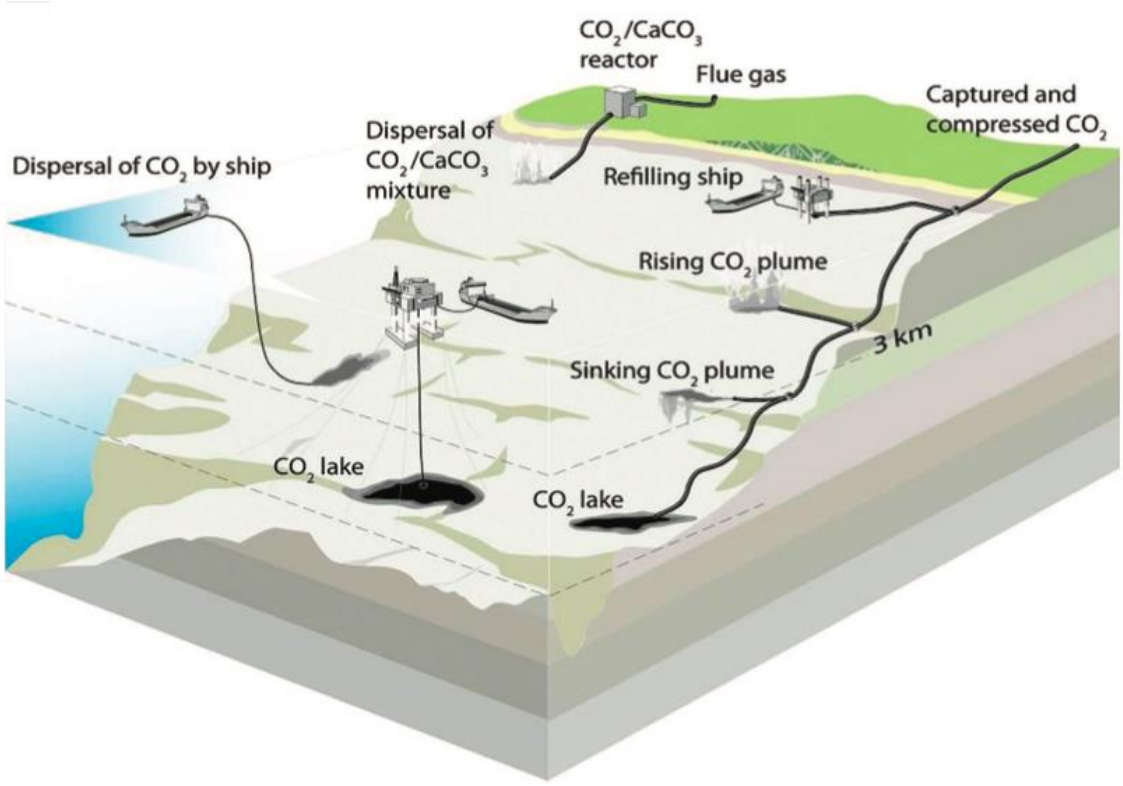

Figure 3-2: Strategies for ocean carbon sequestration (Adams and Caldeira, 2008)

At typical pressure and temperature conditions in the ocean, pure CO_2 would be a gas above approximately 500 m and a liquid below that depth (Herzog, 1998). In seawater, the fluid would be positively buoyant (i.e., it will rise) until about 3000 m, but negatively buoyant (i.e., it will sink) below that depth. In seawater-CO_2 systems, CO_2 hydrates can form below about 500 m depth, depending on the relative compositions. CO_2 hydrate is a solid with a density of about 10 % greater than that of seawater.

The problem of the direct ocean storage method is the reduction of the pH of the ocean. When CO_2 is added to the seawater, the water's pH-value decreases, i.e., water becomes acid with potentially detrimental marine life effects.
The release of CO_2 in the ocean could be done in an unconfined or in confined way. The simpler concept is an unconfined release leading to a buoyant droplet plume, while the objective of a confinement water volume is to produce a concentrated CO_2-seawater mixture such that negative buoyancy will produce a sinking plume (in the open ocean) or gravity current (along a sloping seabed) (Adams et al., 1995).
For an unconfined release of CO_2 in the ocean, plume dilution will result in a minimum pH of about 6, while for a confined release, the minimum pH could be as low as about 4.5 (Adams et al., 1995). Away from the injection point, the perturbations will diminish as the CO_2 concentrations decrease by dilution. The possibility of hydrate formation may cause additional impacts.
By considering a business-as-usual scenario, i.e., continued emissions of CO_2 to the atmosphere followed by uptake across the air-sea surface, this will induce a consequent reduction of near-surface pH in the long term in large parts of the world. This means that the ocean will approach natural variability limits and may go beyond pH acceptance limits for marine biota. Considering a large scale dissolution of CO_2 in the sea, the adverse effects will be deeper in the water column, but would reduce the impact in the near-surface waters. Most of the biological production, including that part important for commercial fisheries, occurs in the upper layer (Herzog, 1998).
Impacts would occur principally to non-swimming marine organisms residing at depths of about 1,000 m or greater. Their magnitude will depend on both the level of pH change and exposure duration (Herzog, 1998). However, available data suggest that pH change impacts can be completely avoided if the injection is properly designed to diffuse CO_2 as it dissolves.

Today, the injection of CO_2 into seawater has only been investigated in the laboratory, small-scale in-situ experiments, and mathematical models. Larger-scale in-situ experiments have not yet been carried out, and for this reason, this technology has a TRL of 2, as shown in Figure 1-2.

The cost of ocean storage is a function of the distance off-shore and injection depth. By considering a distance of 100-500 km off-shore and an injection depth of 3,000 m, the cost range is 6-31 $/t$CO_2$ stored (IPCC, 2013), including off-shore transportation costs.

3.4 Confined Submarine Carbon Storage

The liquid carbon dioxide can also be stored in glass capsules into the deep seabed, a process called Confined Submarine Carbon Storage (CSCS). By keeping the CO_2 separated from the seawater, the pH of this is not affected. The marine environment risks are lessened since they are only related to the potential breakage of the capsules and the consequent release of CO_2.

Given its intrinsic modularity and small size, the CSCS storage line can be installed close to industrial facilities or CO_2 emission sources located on the coastline, provided a proper marine storage location within 200 km. This is because of the widespread availability of the raw materials required for the capsules production (Caserini et al., 2017).

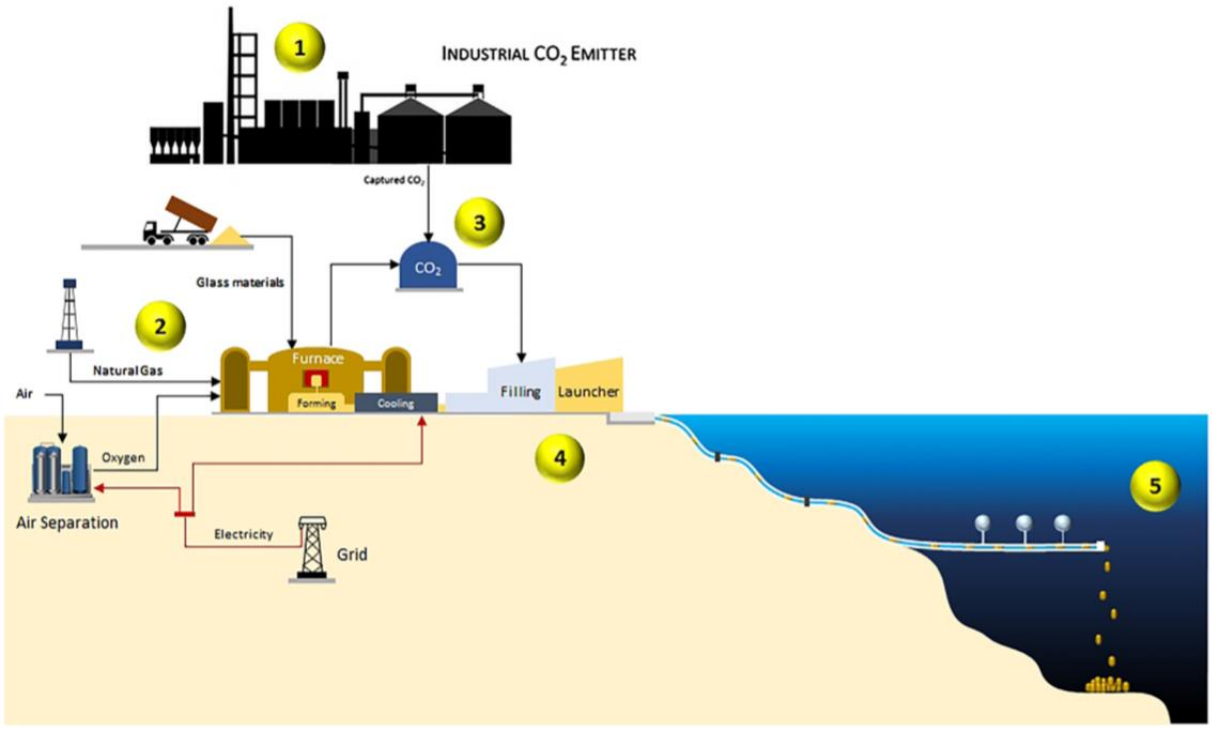

Figure 3-3: Scheme of the Confined Submarine Carbon Storage process (Caserini et al., 2017)

In Figure 3-3, the different phases of the process are summarized. Initially (1) in Figure 3-3, the emitter setup the CO_2 capture system. Then (2) there is the production of glass capsules. After this (3), the CO_2 is collected from the emitter and capsules production. During the filling of the capsules (4), a certain amount of sand is inserted in them to guarantee the desired rate of fall speed after their release into the sea before the seabed deposition. Finally, (5) the filled capsules are transported to the sea and here released.
The availability of space in the seabed for submarine CO_2 is a minor issue for developing this technology. The suitable areas are requested to have large deep seabed available close to the shores, like the Mediterranean and Black seas assessed by Caserini et al. (2017).
Monitoring is fundamental both for risk assessment and risk management operations. Critical aspects of monitoring are: the integrity of the capsules, the overall environment status of the storage site, and in the occurrence of CO_2 loss, the associated environmental effects.
A problem of this method is related to the breakage of the glass capsules, that may occur either inside the pipeline or in the deployment site on the seafloor, consequently causing a CO_2 leakage. This may also happen in the long-term due to natural events, like submarine earthquakes, or other ongoing human activities that can potentially threaten the storage site's integrity.
Right now, this technology is in the formulation process, so it has a TRL of 2.
The overall costs of the CSCS plant amount to 17.5 $/t$CO_2$ stored and a range of 12-30 $/t$CO_2$, potentially competitive with the other conventional storage technologies (Caserini et al., 2017).

3.5 Enhanced Weathering of Limestone

3.5.1 Scheme of the technology

The method proposed by Caldeira and Rau, called Enhanced Weathering of Limestone (EWL), consists of enhanced carbonate dissolution to capture and sequestering carbon dioxide.

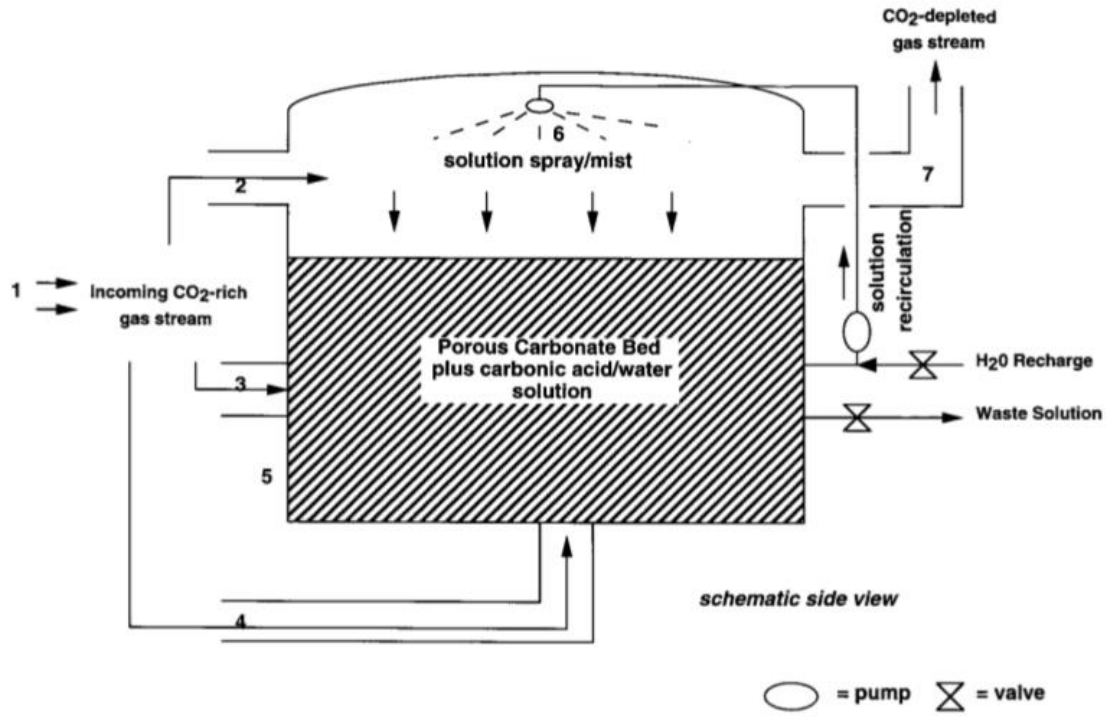

Figure 3-4: An example of a possible EWL reactor design (Caldeira and Rau, 2000)

In Figure 3-4, an example of EWL reactor design is illustrated. A CO_2-rich gas stream (1) enters the reactor vessel (5) by one or more entryways (e.g., 2, 3, or 4). The gas stream passes over (2) or through (3, 4) a wetted, porous bed of calcium carbonate (e.g., limestone) particles within the reactor. This carbonate mass is sprayed (6) and wetted with and partially submerged in a water/carbonic acid solution, which is undersaturated with respect to bicarbonate ion. The arrangement process exposes the incoming gas to a large surface area of water/solution in the form of droplets and wetter carbonate particle surfaces in (5), facilitating hydration of the entering CO_2 to form a carbonic acid solution within the reactor. CO_2-depleted gas then exits the reactor (7) (Rau and Caldeira,1999). The different steps and the reactions are:

1. The CO_2-rich effluent gas stream is hydrated with water to form carbonic acid:

$$CO_2 + H_2O \implies H_2CO_3 \tag{3.1}$$

2. The hydrated CO_2 is then reacted with a mineral carbonate (limestone) to form Ca^{2+} and bicarbonate ion in solution:

$$H_2CO_3 + CaCO_3 \implies Ca^{2+} + 2HCO_3^- \tag{3.2}$$

The net reaction being:

$$CO_2 + CaCO_3 + H_2O \Longrightarrow Ca^{2+} + 2HCO_3^- \quad (3.3)$$

The basic chemistry calculation for this method is reported in Table 3-1.

Table 3-1: Working parameters for the EWL method (from Caldeira and Rau, 2000)

EWL	Initial seawater in equilibrium with atmosphere (A)	In equilibrium with 0.15 atm CO_2 (B)	In equilibrium with 0.15 atm CO_2 and Calcite (C)	Degassed to seawater W_{cal} (D)	Diluted with 100 parts seawater (E)	Degassed to equilibrium with atmosphere (F)
pCO_2 (∝atm)	350	150000	150000	35339	415	350
∑Alk (∝eq kg^{-1})	2314	2314	14808	14808	2438	2438
∑CO_2 (∝mol kg^{-1})	2047	7459	19921	15893	2184	2149
$CO_{2(aq)}$(∝mol kg^{-1})	12	5143	5143	1212	14	12
HCO_3^- (∝mol kg^{-1})	1844	2315	14749	14563	1983	1928
CO_3^{2-} (∝mol kg^{-1})	191	1	29	118	187	209
Ca^{2+} (mmol kg^{-1})	10.12	10.12	16.37	16.37	10.18	10.18
W_{cal}	4.14	0.02	1	4.14	4.14	4.56
pH	8.22	5.69	6.5	7.12	8.18	8.24

3.5.2 Pros and cons

Anthropogenic CO_2 released to the atmosphere will eventually be buried as carbonate sediments through several steps occurring in very long time scales. The CO_2 emitted into the atmosphere equilibrates with the surface ocean in less than one year. This dissolved CO_2 is mixed from the surface to the deep sea on the scale of about 300 years. The acidity produced by the dissolved CO_2 is partially neutralized by the dissolution of carbonate minerals on the scale of about 6,000 years, allowing the ocean to absorb more CO_2 from the atmosphere. Ultimately, on the scale of 10^5 years, enhanced silicate-rock weathering will provide the cations needed to bury the anthropogenic CO_2 as carbonate sediments (Caldeira and Rau, 2000).

Injection of CO_2 directly into the deep sea bypasses the surface-equilibration and mixing-to-deep-sea steps. The carbon-dissolution method largely avoids these steps and the natural carbonate dissolution step by dissolving carbonate minerals at the site of CO_2 production. The carbonate dissolution would eventually occur naturally on land and in the sea, but throughout many millennia.

It is then advantageous to place water and mineral carbonate in direct contact with waste gas stream whose pCO_2 is commonly several orders of magnitude higher than that of the atmosphere (e.g., flue gas pCO_2 at 0.15 bar vs. atmospheric $pCO_2 = 3.7 \times 10^{-4}$ bar). This would allow $CO_{2(aq)}$ and carbonic acid to form faster and in concentrations much higher than it would naturally occur in water in contact with the atmosphere.
The increase in alkalinity from the Ca^{2+} would tend to cause dissolved inorganic carbon in the form of HCO_3^-, which cannot directly interact with the atmosphere. In this way, power plant CO_2 could be effectively stored in the oceans, mainly as HCO_3^- (Caldeira and Rau, 2000).

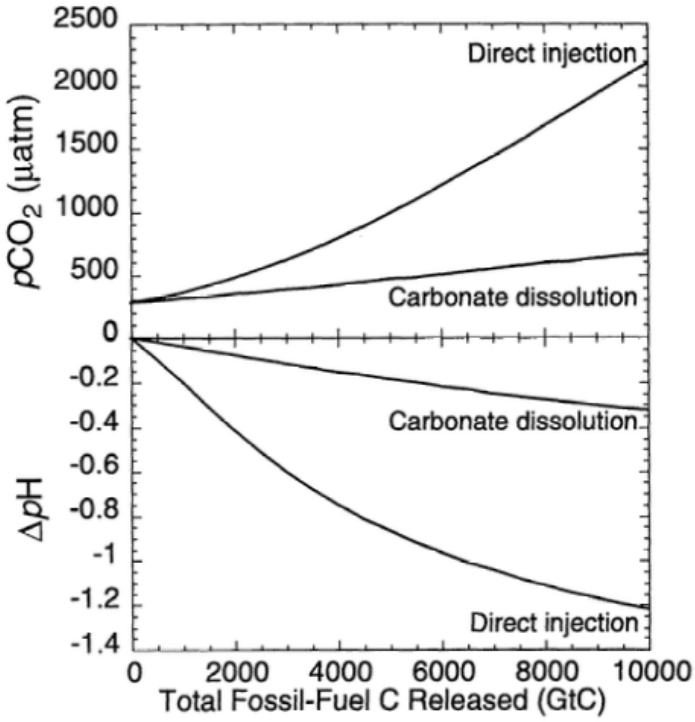

Figure 3-5: Comparison of the effects of direct CO_2 injection and carbonate dissolution method 1,000 years after injection (from Caldeira and Rau, 2000)

Figure 3-5 presents a comparison between the direct CO_2 injection and the carbonate-dissolution technique, both released in the deep ocean, 1,000 years after injection. With the direct injection method, over 45% of large amounts of anthropogenic CO_2 release it degasses back to the atmosphere after 1,000 years. With the carbonate-dissolution process, less than 15% of the initially released CO_2 degasses back to the atmosphere. Also, the pH changes are way different in the two methods. With direct injection after 1,000 years, the ΔpH is -1.2, while with EWL, this value is only ~0.3.

This method is geochemically and environmentally advantageous because the dissolution of carbonate minerals neutralizes CO_2-acidity and mainly converts CO_2 to a form that does not exchange with the atmosphere. EWL largely obviates the need for a large amount of energy to separate and inject CO_2 deeply into the ocean.

EWL is an attractive option for CO_2 mitigation for different reasons:

- the required reactants are relatively inexpensive, abundant, and environmentally benign;
- the technology is relatively simple, low-cost, and applicable to power plant retrofitting, even in developing countries;
- the storage is effective and long-term;
- the waste products are stable and may have net positive environmental effects for marine life.

A problem with this method is that a very high amount of water is needed and many minerals. 3.8x103 tonnes of water are required to discharge with a pH similar to the natural one, an amount too high from a physical and economic point of view since it requires vast reactors.

Another problem is that EWL requires a lot of minerals, so the method is suitable in places close to a quarry to limit transportation costs.

There are only laboratory tests about this option, so it has a TRL of 2.

The cost per tonne CO_2 sequestered ranges from about 18 $ to 128 $, including the transport of minerals and water (Caldeira and Rau,1999).

3.5.3 Case study

Kirchner et al. (2020) evaluated the performance of the biggest EWL-reactor to date installed at a coal-fired power plant in Germany. Depending on the gas flow rate, approximately 55% of the CO_2 could be removed from the flue gas. During all their performed experiments, they observed elevate Total Alkalinity (TA) values in the product water. In general, TA increased from 2 to 5.6 mM due to EWL treatment. This increase was higher than those observed in lab-scale experiments performed by Chou et al. (2015) and Rau (2010), who achieved TA increases of <0.5 and <2 mM, respectively. Their results also show that the flue gas and water suspension's contact time within the reactor was too low, and reaction (3.3) was not completed in the regular experiments.

Although EWL increases the TA of the product water, the pH decreases during the

treatment. In Kirchner et al. 's standard experimental setup, the pH values of the product water were between 6.6 and 7.5 (seawater pH: about 8.0). If the product water that left the EWL reactor was stirred for equilibration of CO_2 with the atmosphere, they observed a substantial increase in pH to values of 8.4 within 7 hours.
They concluded that EWL could be used for safe and long-term storage of CO_2, at locations where limestone and water availability is high. The resulting product water could be safely disposed of in the marine environment taking into account the possible impact of increasing TA and decreasing pH.

Kirchner et al. (2020) also studied how EWL-derived water impacts the southern North Sea's carbonate chemistry. They explored different scenarios considering different gas streams, one of a very small (60 kW) combined heat and power plant and a coal-fired power plant (750 MW). In the first scenario, the pH is expected to decrease by maximal 0.1, whereas Ω_{cal}, the saturation state of calcite, increases by 0.6. The saturation state measures the thermodynamic tendency for the mineral calcium carbonate to form or dissolve. A saturation state greater than 1 indicates supersaturation and the risk of precipitation, while value less than 1 indicates undersaturation with instability favoring dissolution (NECAN, 2013).
In the other two scenarios with the scrubbing gas stream of a coal-fired power plant, on the contrary, the discharge of the EWL-derived water has substantial effects on the marine biota because of significant alterations on pH and Ω_{cal} of 1 and 8, respectively. Part of the CO_2 dissolved in the EWL-derived water will degas due to the higher partial pressure with respect to the atmosphere, increasing the marine pH. Close to the discharge site, the abiotic precipitation of carbonates could be a consequence, which would lower EWL-efficiency in CO_2 storage capacity.
Kirchner et al. (2020) considered to discharge the solution in shallow water, and in this way, 50% of the captured CO_2 remained in the North Sea. In contrast, the other 50% re-entered the atmosphere at the end of the simulations due to the degassing and carbonate mineral precipitation.

A technology called Enhanced Pressurized Weathering of Limestone (EPWL) has been proposed by Cappello and Ross Morrey to reduce the amount of water needed and is presented in the following chapters.

Chapter 4: ANALYSIS OF A NEW TECHNOLOGY: ENHANCED PRESSURIZED WEATHERING OF LIMESTONE (EPWL)

The technology considered in this study for the storage of CO_2, proposed by Cappello and Ross Morrey (2020), is called Enhanced Pressurized Weathering of Limestone (EPWL). It consists of a plant in which the CO_2 taken from power plants reacts with water and carbonate according to the reactions (3.1, 3.2, 3.3) discussed in chapter 3.5 about the EWL, and then it is discharged in the ocean in a system that works at high pressure.
In EPWL, after the initial mixing among water, CO_2, and micronized carbonate mineral, the carbonate mineral dissolution reactions happen inside a pipe under a condition of progressively increased pressure. The tube is located between the coast and the deep sea, so variable increasing pressure is generated inside the pipe due to the sea's hydrostatic pressure; this enhances the solubility of limestone and increases the partial pressure of CO_2. In this way, the production of bicarbonates is promoted until the solution reached the discharge point depth.

A schematic representation of the technology is displayed in Figure 4-1.

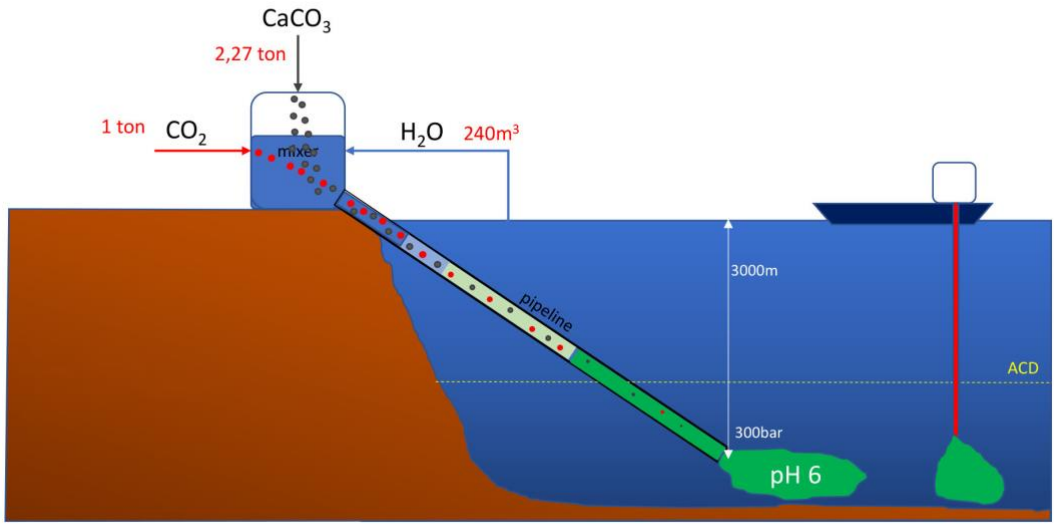

Figure 4-1: Schematic representation of the EPWL technology (Cappello and Ross Morrey, 2020)

The CO_2 can be taken from a CO_2 rich-flue gas by scrubbing it with seawater, or can be used as a flux of pure CO_2 since the technologies of CO_2 capture are already developed. This second option is the one considered for the analyses of this study.

The process could use the two forms of calcium carbonate ($CaCO_3$):

- Aragonite: is a material formed by the carbonate that crystallizes in a bi-pyramidal diamond class and is a polymorph of calcite. This material can be found in many marine organisms, e.g., in the shells, corals, and coral sands.
- Calcite: is a material formed by the carbonate that crystallizes in a trigonal class. It can be found in limestone and dolomite deposits.

Once the carbonate is dissolved in the reactor in the form of Ca^{2+} and $2(HCO_3^-)$ is at a depth below the Carbon Compensation Depth, the calcite's risk will precipitate is absent. The need to discharge the effluent below this depth is only necessary if the calcite has not been completely dissolved. Then the technology ensures to dissolve the calcite before the discharge or along the pipe.

The stoichiometric amount of water required, according to Reaction 3.3, to dissolve 1,000 kg of CO_2 and 2,270 kg of carbonate mineral (at ambient pressure and water temperature = 5°C) is 409 kg. In this case, using the software PHREEQC (the software is explained in detail in chapter 5.1), it is possible to assess that the pH at this equilibrium is very low, i.e., 2.7. To increase the effluent's pH and favor the reaction in real conditions, it is thus necessary to use an excess of water respect to the one required by Reaction 3.3. The amount of water needed at atmospheric pressure is very high, on the order of thousands of m^3 per tonne of CO_2. Thus, the proposal of a pressurized reactor aims to reduce the amount of water needed to remove the CO_2 from the stream and accelerate the carbonate mineral's dissolution. Since the process is done inside a pipe with a specific length, it is necessary to evaluate if the equilibrium is reached before its end. Thus, the kinetics of the reaction should be considered.
The amount of water needed in the pipe for the complete dissolution of the $CaCO_3$ depends on the quantity of reactants and on the pH that could be acceptable at the discharge point. It could be assessed by PHREEQC considering the solution at the equilibrium just before the discharge point. The adequate residual carbonate mineral and pH depend on the possibility that carbonate mineral after the discharge could complete the dissolution.
There are thus two different scenarios:

- the pipe discharges the effluent below the Carbonate Compensation Depth (CCD) ;
- the pipe discharges the effluent above the CCD

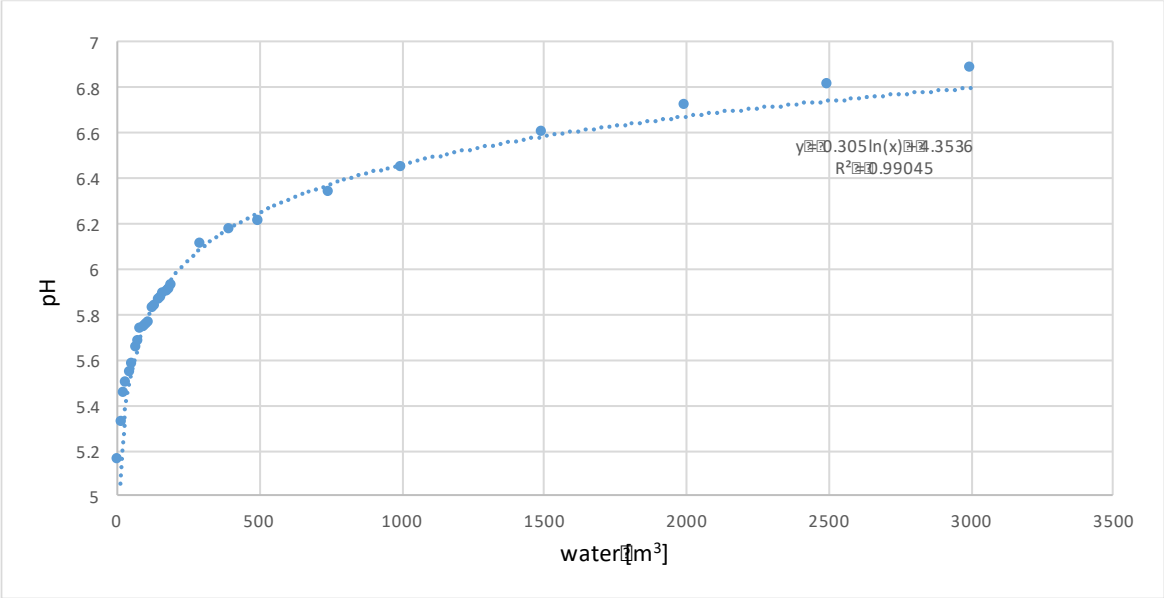

Figure 4-2: pH equilibrium as a function of water quantity for the complete dissolution of 2,272.2 kg of $CaCO_3$ and 1,000 kg CO_2

Figure 4-2 reports the quantitative analysis done with the software PHREEQC of pH equilibrium as a function of water quantity for the complete dissolution of 2,272.2 kg of $CaCO_3$ calcite and 1,000 kilograms of CO_2 in generic seawater at the working pressure of 300 bar. The Italian legislation allows the discharge of water in the sea with a pH between 5.5 and 9.5. This technology could then be used with a water load higher than 500 m_3 of seawater per tonne of CO_2.

Once CO_2 has reacted with limestone and water forming bicarbonates, CO_2 is sequestered in the sea for an undefined time in the form of bicarbonates until a variation of pressure or pH does not alter the solubility conditions of the limestone.

It is crucial to understand how calcite dissolution behaves for avoiding precipitation. In the following sections, the factors that influence the dissolution of calcite in seawater will be briefly summarized.

4.1 Calcite dissolution kinetics

The dissolution rate of calcite with respect to the saturation rate is usually modelled by a simple empirical equation (Gledhill and Morse, 2006):

$$R = k(1 - \Omega)^n \tag{4.1}$$

where:

- *R* is the rate (mol m^{-2} h^{-1});
- *k* is an empirical constant;
- *n* is a constant describing the order of the reaction;
- Ω is the saturation state of mineral carbonates, defined as the *in situ* calcium and carbonate ion concentrations divided by the apparent product solubility.

The following equation defines the saturation state:

$$\Omega = \frac{[Ca^{2+}]\,[CO_3^{2-}]}{k'_{sp}} \tag{4.2}$$

where:

- $[Ca^{2+}]$ is the calcium ion concentration (mol m^{-3})
- $[CO_3^{2-}]$ is the carbonate ion concentration (mol m^{-3})
- k'_{sp} is the product solubility for calcite at the temperature of interest

Equation 4.1 fits well with the real conditions in the far-from-equilibrium conditions, i.e., when mineral carbonates' saturation state is low. In this case, a linear relation between dissolution rate and saturation state is assumed, so the order of the reaction, *n*, is equal to 1.
The situation is different when the equilibrium is approached. In the near-equilibrium condition, the rate is highly nonlinear, so many authors proposed other models to simulate calcite dissolution kinetics based on experimental data.

4.2 Factors influencing the dissolution of calcite in seawater

It is fundamental to define the different factors that influence this process to define a system to model the dissolution of calcite in seawater,

The concentration of dissolved carbon dioxide is strongly dependent on seawater pH. If pH increases, the proportion of dissolved CO_2 falls, while bicarbonate reaches a maximum at a pH around 7-8, as shown in Figure 4-3.

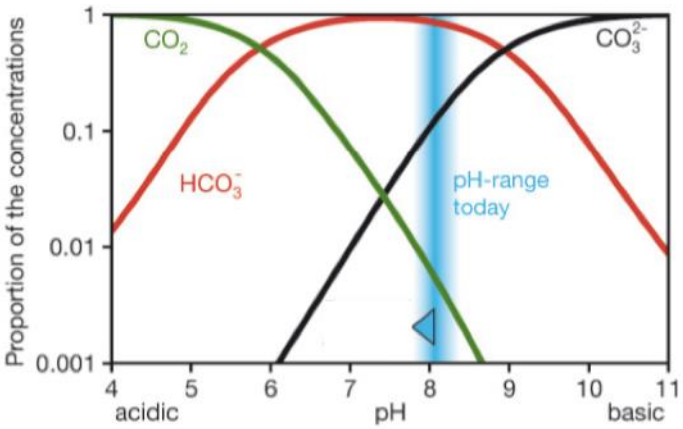

Figure 4-3: Proportion of various carbon species as a function of pH and expected change of pH in virtue of ocean acidification (Tannenberg, 2009)

Shifting the equilibrium to carbonate ions causes uptake of atmospheric carbon dioxide to maintain a constant ratio of $pCO_2/CO_{2,aq}$.

In section 3.1, CO_2 solubility in seawater increases with increasing pressure and decreases with increasing temperature. Thus the best conditions for having a more significant dissolution are higher pressure and lower temperature. These conditions are also valid for carbonate dissolution, and also an increase in CO_2 concentration pushes the equilibrium of the reaction 3.3 to the right, producing more products and consuming more reactants.

Many experiments pointed out that the laboratory results are faster than the ones conducted *in-situ*, which is due to natural inhibitors that slow the natural process. Lea et al. (2000) measured the influence of carbonate, manganese, and strontium ions on calcite dissolution.
They stated that the dissolution rate and etch-pit morphology are highly dependent on the presence of cationic impurities and CO_3^{2-} ions in solution. The dissolution rate and etch-pit morphology changes are kinetically driven by the contact rates of ion pairs at the calcite surface. Kink propagation is retarded by the absorption of ions or ion pairs along with the pipe and single-kink sites. The absorbing species can influence the formation of double-kink sites and block, or at least inhibit the dissolution of single-kink sites.
At low concentrations, delay of double-kink formation is the dominant process. At higher concentrations, delay of single-kink dissolution along the step is dominant. A sharp change in step-edge migration velocities is projected at the threshold concentration where rate control shifts from double-kink formation to single-kink dissolution.

Ruiz-Agudo et al. (2009) investigated the influence of electrolytes on the kinetics and the calcite dissolution mechanism. Experiments were carried out far from equilibrium by passing alkali halide salt (e.g., NaCl, NaF, NaI, KCl, and LiCl) solutions over calcite cleavage surfaces.
The obtained result is that all the tested electrolytes enhance the calcite dissolution rate. The effect and its magnitude are determined by the nature and the concentration of the electrolyte solution.
At high ionic strength, salts with an expected anion yield similar dissolution rates, increasing in the order $Cl^- < I^- < F^-$ for salts with a common cation due to increasing mobility of water around the calcium ion.
This is because highly hydrated ions increase the etch pit nucleation density by up to one order of magnitude compared to the pure water. This may be related to reducing the energy barrier for etching pit nucleation due to the disruption of the surface hydration layer.

Xu and Higgins (2010) investigated the effects of magnesium concentration and solution saturation on near-equilibrium calcite dissolution kinetics and surface morphology. Dissolved Mg^{2+} displayed negligible inhibitory effects on calcite dissolution, even at concentrations of 10^{-4} molal (m). Upon introducing 10^{-3} m of Mg^{2+}, the solution saturation state with respect to calcite, Ω, acted as a "switch" for magnesium inhibition whereby no significant changes in step kinetics were observed at $\Omega_{calcite} < 0.2$, whereas a sudden inhibition from Mg^{2+} was activated above this level.
As a result of their study, Higgins and Xu assessed the magnesium inhibitory effects on near-equilibrium calcite dissolution processes. The existence of the *Ω-switch* in magnesium inhibition indicates that the relationship between dissolution kinetics and saturation state is nonlinear in the presence of magnesium impurities.

In conclusion, the most substantial influence on the calcite dissolution rate is not the salt content but the temperature and the CO_2 partial pressure. Ionic strength strongly correlates with an inhibition of dissolution rate beyond the specific effects of calcium and magnesium. Magnesium showed only a minor inhibitory effect, whereas calcium increased the rate constants (Gledhill and Morse, 2006).

Chapter 5: DESIGN OF THE MAIN PARAMETERS OF EPWL

5.1 Software used

Most of the simulations in this work have been done using the software PHREEQC Version 3. This computer program, developed by the U.S. Geological Survey (USGS, 2020), is written in the C++ programming language, and it is designed to perform a wide variety of aqueous geochemical calculations.
It is based on the equilibrium chemistry of aqueous solutions interacting with minerals, gases, solid solutions, exchangers, and sorption surfaces. It can model kinetic reactions and one-dimensional transport.
PHREEQC can be used as a speciation program to calculate saturation indexes, the distribution of aqueous species, and the density and the specific conductance of specified solution composition.

The other software used in this work is Visual Plume 4th Edition (Frick et al., 2003). This computer application simulates single and merging submerged plumes in arbitrarily stratified ambient flow and buoyant surface discharges.

5.2 Initial conditions

It is necessary to describe the characteristics of the considered seawater to perform the simulations to design the EPWL, particularly the pH, the temperature, and the mineral composition, i.e., all the factors that affect the dissolution of $CaCO_3$.

5.2.1 pH

According to Sarmiento and Gruber (2006), seawater pH is typically in the range between 7.5 and 8.4, with substantial regional variations. For the following calculations, an average value of 8 has been then considered. It is worth remembering that seawater pH is decreasing due to the increase in atmospheric CO_2.

5.2.2 Temperature

The dissolution of $CaCO_3$ in water increases with increasing pressure and decreasing temperature (Shariatipour et al., 2016). To understand this effect, simulations have been done considering a vertical pipe of 3000 m inside the ocean, in which the water has the velocity of 1m/s, and 360 m_3 of water are used to obtain a final pH of 6 at least, according to Figure 4-2.

These simulations have been done for different temperature values to see this parameter's influence on the final calculations. As a result, it has been evaluated the amounts of Ca_{2+} in solution, one of the product of Reaction 3.3 that derives from the dissolution of $CaCO_3$ in seawater.

This amounts of Ca_{2+} in solution along the pipe increases with the depth at different temperature values, as shown in Figure 5-1.

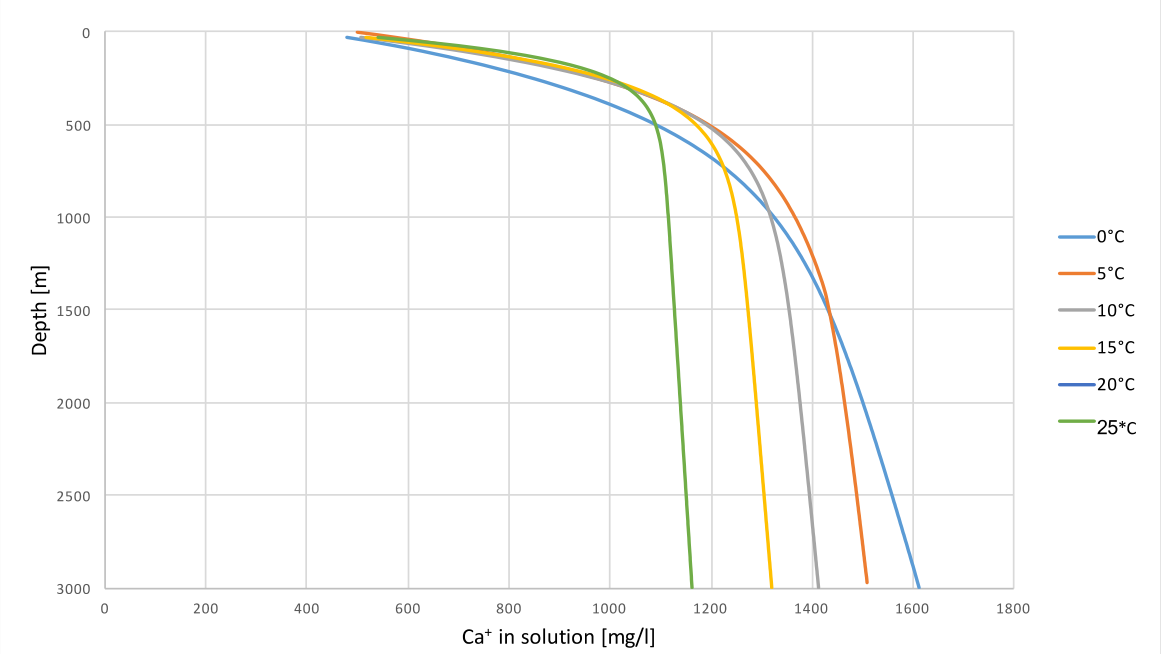

Figure 5-1: Ca_{2+} in solution along a 3000 m pipeline for different temperature values

Based on this graph, it is clear that as the temperature decreases, the amount of dissolved $CaCO_3$ increases, and so the amount of Ca in solution.

For the following analyses, a temperature value of 5°C was chosen.

5.2.3 Mineral composition

Another factor that influences calcite's dissolution is the mineral composition of seawater, as already explained in detail in chapter 4.2.

The six most abundant ions of seawater are chloride (Cl^-), sodium(Na^+), sulfate(SO_4^{2-}), magnesium (Mg^{2+}), calcium (Ca^{2+}) and potassium (K^+). By weight, these ions make up about 99 percent of all sea salts. The amount of these salts in a seawater volume varies because of the local addition or removal of water (e.g., through precipitation and evaporation). The salt content in seawater is indicated by salinity (S), which is defined as the amount of salt in grams dissolved in one kilogram of seawater and expressed in parts per thousand. Salinity in the open ocean has been observed to range from about 34 to 37 parts per thousand (USGS, 2020).

The calculations of this study used the mineral composition presented by Lyman and Fleming (1939), reported in Table 5-1.

Table 5-1: Mineral composition of seawater (Lyman and Fleming, 1939).

Salt	**g salt/kg water**
Cl	18.9799
Br	0.0646
SO_4	2.6486
HCO_3	0.1390
F	0.0013
Ca	0.4001
Mg	1.2720
K	0.3800
Sr	0.0133
Na	10.5561
H_3BO_3	0.0260
SUM	**34.4816**

5.2.4 Calcite dissolution kinetics

For what concerns the calcite dissolution kinetics, the formula that is implemented in the database of the software PHREEQC has been used, in which the rate of dissolution depends on the saturation index of $CaCO_3$, that is explained in detail in chapter 5.5, the amounts of water and CO_2, the pH of the solution and a surface area index that needs to be defined before the calculation and depends on the size of the calcium carbonate particles. The value of the surface area index decreases as the reaction proceeds. The particles

decrease their size until they are completely dissolved. This is simulated in the software through the ratio between the initial moles and the current ones, which becomes lower at each iteration.

The formula used to simulate this process is:

$$surface\ area\ index = SA_0\ m_0 \left(\frac{m}{m_0}\right)^a \tag{5.1}$$

where:

- m_0 are the initial moles
- m are the current moles at each step
- SA_0 is the initial surface area index
- a is a parameter defined by the user.

SA_0 corresponds to the initial surface area index of calcite particles. Equation 5.2, proposed by Subhas et al. (2015), has been used to calculate it for different particle sizes.

$$SA_0 = \frac{6}{\rho \cdot \bar{d}} \tag{5.2}$$

where $\rho = 2.63\ g/cm^3$ is the assumed density of calcite and $\bar{d}$ is the mean grain diameter of the sieved fraction.

The software requires this parameter in terms of cm^2/mol. This value, that is in cm^2/g, was then multiplied by the molecular weight of $CaCO_3$, 100.092 g/mol.

In the further calculations were considered three different particle sizes: 25,50 and 100 μm, typical commercial values, and their respective surface area indexes in cm^2/mol are listed in Table 5-2.

Table 5-2: Initial surface area indexes used in the simulations

∝m	Surface Area [cm^2/mol]
25	9.00E+06
50	4.00E+06
100	2.00E+05

Since the surface area index is crucial for the reaction's kinetic, it is necessary to calculate its value at the end of the pipe, and so the size of the particles that leave the tube. In the case of discharging below the CCD, it is important to assess if the particles are sufficiently small to avoid their precipitation. In contrast, in the case above the CCD, the surface area index is necessary to define the reaction inside the reactor's response.

The surface area index at the beginning of the simulation is $surface\ area\ index = SA_0 m_0$, since $m_0 = m$. By looking at the moles at the end of the simulation, it is possible to calculate the discharge point's surface area index. By having the index values at the beginning and the end of the simulation, the following proportion has been used to find the particle size after discharge point:

$$R_f = A_f \cdot R_i / A_i \qquad (5.3)$$

where:

A_i = surface area index at the beginning

A_f = surface area index at the discharge point

R_i = initial particles size

R_f = final particles size.

In this way, the calcite's particle size at the end of a vertical 4,500 m pipe has been evaluated. The velocity of water inside the pipe is 1 m/s. The values for different amounts of water are reported in Table 5-3 and 5-4 for two different initial particles size, respectively, for 25 and 50 μm.

Table 5-3: Particle size of calcite at the end of a vertical 4,500 m pipe for different amounts of water (initial particles size = 25 μm)

Water (m^3)	Initial particle size (μm)	Final particle size (μm)
500	25	17.05
1000	25	14.16
1500	25	12.12
2000	25	11.10
2500	25	10.48
3000	25	9.66
3500	25	8.96

Table 5-4: Particle size of calcite at the end of a vertical 4,500 m pipe for different amounts of water (initial particles size = 50 μm)

Water (m^3)	Initial particle size (μm)	Final particle size (μm)
500	50	34.22
1000	50	28.96
1500	50	24.97
2000	50	23.18
2500	50	22.15
3000	50	20.85
3500	50	19.75

5.3 Preliminary analysis on $CaCO_3$ dissolution

A preliminary analysis has been done in order to evaluate the dissolution curve of 2,270 kg of $CaCO_3$ and 1,000 kilograms of CO_2 as a function of pH in the effluent at 5°C and fixed pressure of 300 bar for different amounts of water.
According to the Italian legislation, an effluent discharged in the water must have a pH higher than 5.5. For the further analysis, it has been considered an amount of water of 360 m_3 to respect a pH in the effluent higher than 6, as derived from Figure 4-2.
The results of these simulations are shown in Figure 4-2. They have not been done considering the kinetics of the reaction but only the product at equilibrium.

5.4 Kinetics analysis

The work's objective was then to evaluate the amount of water and the length of the pipe, which is needed to dissolve all the 2,270 kg of $CaCO_3$ before its end.
By considering a particle size of 100 μm, the amounts of calcite dissolved in seawater in a vertical 3,000 m pipe, which corresponds to an absolute pressure of 300 bar, were calculated for different amounts of seawater. The pressure in the simulations increases linearly, considering 1 bar every 10 m.

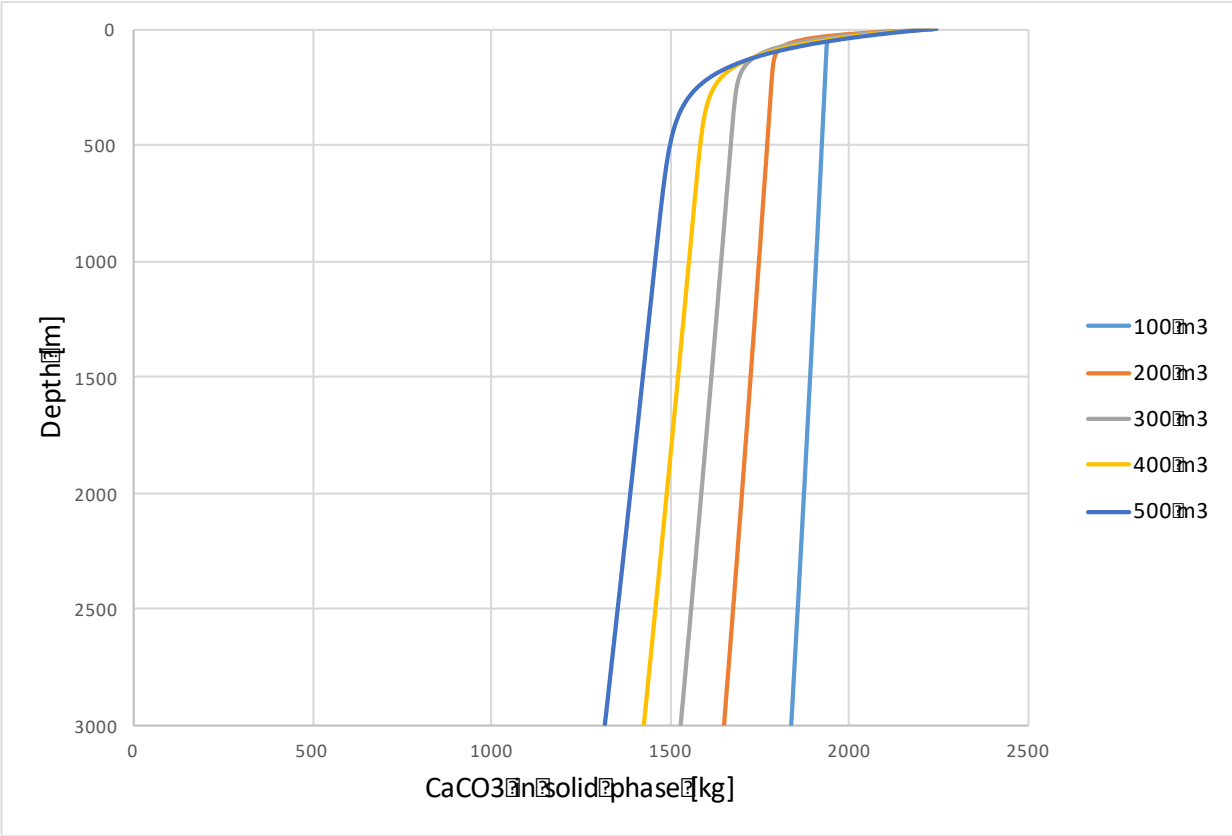

Figure 5-2: Dissolution of $CaCO_3$ in the pipe for different water quantities

Figure 5-2 shows that the dissolution of $CaCO_3$ increases as the amount of seawater increases.

The amounts of unreacted $CaCO_3$ are still very high at the end of the pipe. For example, by considering 500 m_3 of seawater, there is still about 1,400 kg of carbonate minerals in the solid phase at the end of the pipe.

The obtained results show that the amounts of water needed are much larger than the expected one from Figure 4-2, which is 360 m_3 to have a pH of 6. Furthermore, the reaction time needs to be increased since the reaction is slow, so the pipe is required to be longer.

5.5 Water quantities and pipe lengths

The complete dissolution has been obtained by increasing the amount of seawater and the length of the pipe. The velocity of the water inside the pipe is 1 m/s, in order to avoid sedimentation. After this, several calculations were performed to see the amounts of water

needed at different final pressure and different pipe lengths. All these values are obtained considering a particle size of 50 μm because the dissolution is faster.

These results are listed in Table 5-5 and shown in Figure 5-3. The first row of Table 5-5, i.e., the case of discharge at the ocean surface, corresponds to the conditions proposed by Rau and Caldeira (2000), that considered the sequestration of CO_2 with carbonate minerals inside a reactor and then to discharge the mixture in the ocean surface. In this case, the amount of water is very high because the pressure is low. They obtained an amount of water of 3800 m^3 of water/ tonne CO_2, while in this work, the value for 1 bar is 4050 m^3 of water/ tonne CO_2. The two values are not the same because different assumptions have been considered, like the initial particle size, the reaction time, the mineral composition, but they are close, so the results obtained with the software are considered consistent.

Table 5-5: m^3 of water needed to dissolve all the $CaCO_3$ at the end of the pipe for different release depths and pipe lengths

		Pipe length [km]				
		40	**60**	**80**	**100**	**120**
Release depth [m]	**0**	4050	4050	4050	4050	4050
	1000	3800	3700	3600	3300	3200
	2000	3700	3600	3500	3250	3100
	3000	3600	3500	3400	3200	3000
	4000	3500	3400	3300	3150	2900
	5000	3400	3300	3200	2900	2800
	6000	3200	2800	2700	2600	2500
	7000	3100	2700	2600	2500	2300
	8000	3000	2600	2500	2300	2100

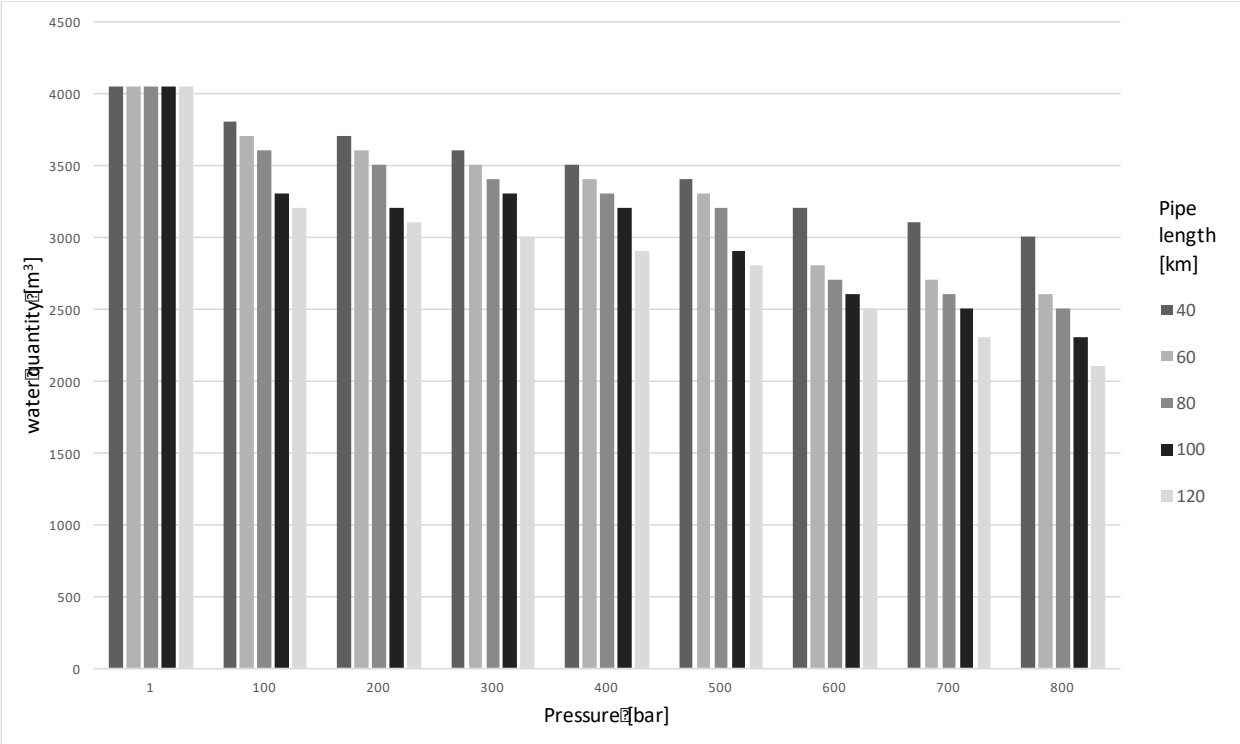

Figure 5-3: m_3 of water needed to dissolve all the $CaCO_3$ at the end of the pipe for different pressures and pipe lengths

Figure 5-3 shows that the amount of water needed decreases as the pressure increases, and the pipe length increases because more reaction time is considered.
Even at 800 bar and considering 120 km of pipe, the cubic meters of water needed is 2100, a very high value even for a plant close to the sea.
The complete dissolution of $CaCO_3$ within the L-pipe requires high water quantities and would not be suitable even in places like Japan, where the ocean becomes very deep, more than 8,000 meters, not far from the coast, in almost 100 km.
By looking at the behavior of a single simulation, for example, in Figure 5-4 regarding the simulation with 80 km of pipe length and final pressure of 400 bar, 3,300 m_3 of water, it is clear that there is a fast dissolution in the first hours. Then the reaction proceeds very slow because the water is almost saturated with respect to calcite, and so the saturation index of $CaCO_3$ is close to 0.
The Saturation Index (S.I.) is a measure of the thermodynamic driving force to the equilibrium state. It is used for determining if the seawater is corrosive or scaling (de Moel et al., 2013).
There are three possible situations regarding this parameter:

- SI < 0 the seawater is undersaturated with respect to calcium so that it will dissolve;
- SI=0 the seawater is in equilibrium with calcium;
- SI>0 the seawater is supersaturated with respect to calcium, and there is the risk that this will precipitate.

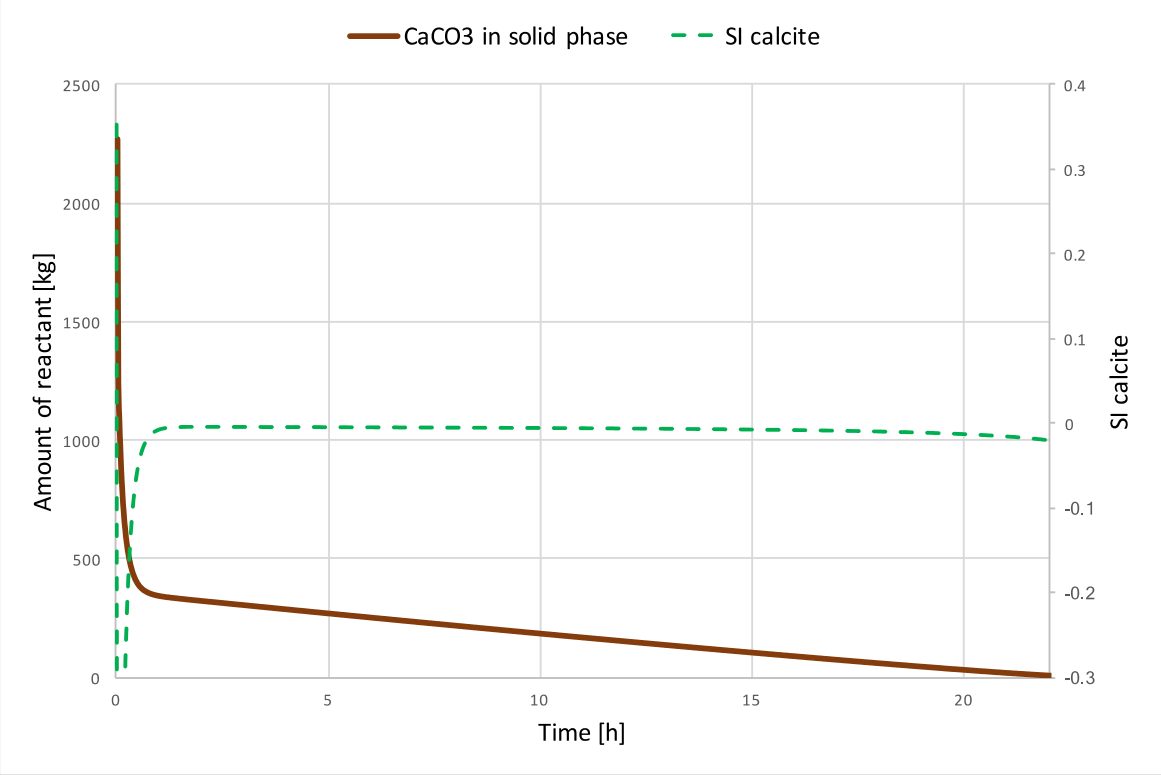

Figure 5-4: Dissolution of $CaCO_3$ with 3,300 m_3 of water in an 80 km pipe at final pressure of 400 bar

For this reason, and also because of the high amount of water needed to obtain the complete dissolution, a new method has been considered, that consists in not achieving a full dissolution, but limiting dissolution inside the pipe only to the further first part and complete the dissolution in open waters. This could only be achieved if the discharge is done below the CCD, where no calcite is preserved, so even if the $CaCO_3$ has not completely dissolved, the risk that it will precipitate is absent.
In this way, the solution is in the initial part of the graph of Figure 5-4, so there is high dissolution in a shorter time.

5.6 EPWL – Discharge below the Carbonate Compensation Depth (CCD)

5.6.1 Scheme of the technology

When the pipe reaches a depth below the Carbonate Compensation Depth (CCD), i.e., the depth in the oceans below which the rate of supply of calcite lags behind the rate of solvation, no calcite is preserved in seawater after the discharge, since it is dissolved by corrosive seawater.

Suppose the discharge from the pipe is below the CCD. In that case, the amount of water in the pipe could be lowered, because the complete dissolution of carbonate mineral before the discharge from the pipe is not needed. This happens because the carbonate mineral that will not react with the CO_2 inside the pipe will anyway dissolve into the seawater, buffering the residual CO_2 inside the plume.

A schematic configuration of this technology is shown in Figure 5-5.

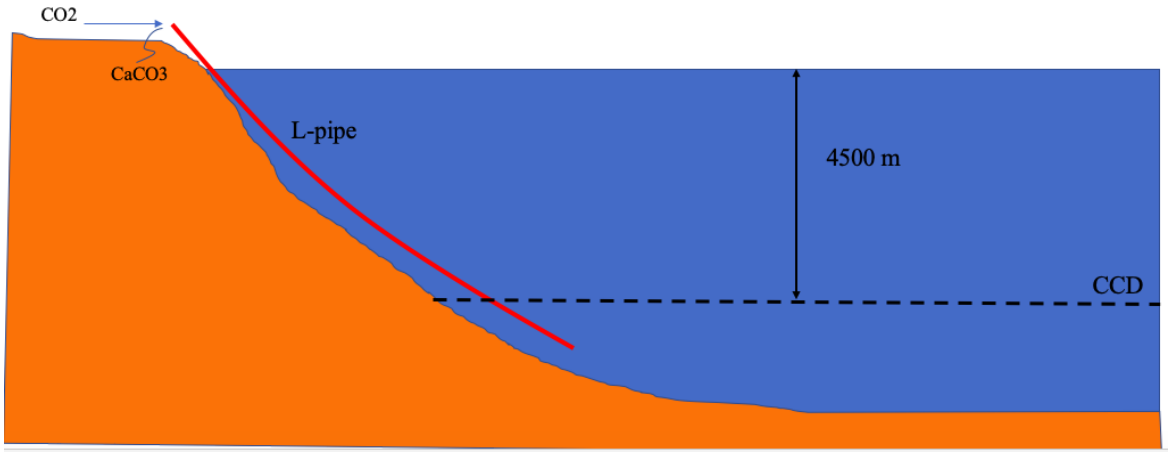

Figure 5-5: EPWL configuration

5.6.2 Carbonate Compensation Depth

At present, the CCD in the Pacific Ocean is about 4,200-4,500 m except beneath the equatorial upwelling zone, where the CCD is about 5,000 m. In the temperate and tropical Atlantic Ocean, the CCD is at approximately 5,000 m. In the Indian Ocean, CCD is at an intermediate depth, between the Atlantic and the Pacific values, at about 4300 meters. The exact level of the CCD depends on the carbonate mineral's solubility, determined by temperature, pressure, and chemical composition of the seawater, particularly the amount of dissolved CO_2. The variation in the CCD depth largely depends on the time since the

bottom water is exposed to the surface; this is called the "age" of the water mass. Thermohaline circulation, a part of the large-scale ocean circulation, is driven by global density gradient created by surfaced heat and freshwater fluxes. It determines the relative ages of the water in these basins. Because organic material sinks from the surface waters into deeper water, deep water masses tend to accumulate dissolved carbon dioxide as they age. The oldest water masses have the highest concentrations of CO_2, and therefore the shallowest CCD. The CCD is relatively shallow in high latitudes, except the North Atlantic and the Southern Ocean regions where downwelling occurs. The downwelling brings young, surface water with relatively low carbon dioxide concentrations into the deep ocean, depressing the CCD.

5.6.3 Assessment of the amount of water required (EPWL)

The software PHREEQC allows assessing, for a different amount of water loaded inside the pipe, the amounts of the reactants (CO_2 and carbonate mineral) remaining at the end of the L-pipe, and the resulting pH of the effluent at the discharge point. Table 5-6 shows the results considering an initial quantity of 1,000 kg of CO_2 and 2,270 kilograms of carbonate mineral, in a 50 km pipe that goes from 0 to -4,500 m inside the ocean.

Table 5-6: Amounts of $CaCO_3$ and CO_2 unreacted and the pH of the effluent at the discharge point, below the CCD

Water (m^3)	**Ureacted $CaCO_3$ (kg)**	**Unreacted CO_2 (kg)**	**pH at the end of the pipe**
100	1778	932	5.6
250	1433	862	5.9
500	1193	552	6.1
1000	874	402	6.4
1500	656	334	6.6
2000	560	269	6.7
2500	505	225	6.8
3000	435	210	6.9
3500	405	206	6.9

Figure 5-6 indicates the amounts of $CaCO_3$ and CO_2 that have not reacted at the end of the pipe for different water quantity, with the respective pH at the discharge point. It was considered a 4,500 m pipe and a 40,000 m pipe, ending both at 4,500 m.

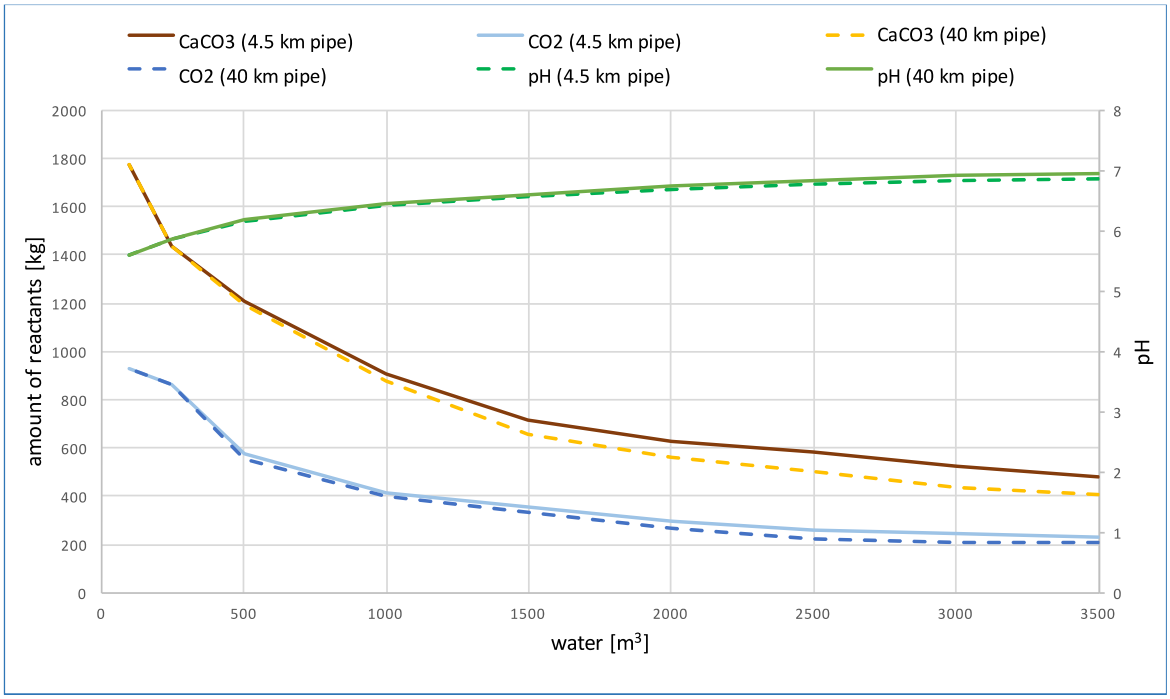

Figure 5-6: Amounts of reactants that have not reacted at different water level in 4,500 m and 40,000 m pipe at 450 bar

Figure 5-6 proves that the length of the pipe, so the reaction time, is not influential as the pressure, since there are only slight differences between the two cases.

The main difference between the EWL and the EPWL is that the effluent of the EWL is already a solution of ionic Ca^{2+} and bicarbonates. In contrast, the effluent of the EPWL is a slurry formed by an ionic solution of Ca^{2+}, bicarbonates, and unreacted carbonate mineral. In the EWL, the ionic effluent composition cannot change but through a CO_2 degassing that would decrease its CO_2 and bicarbonate content through carbonates' precipitation. In the EPWL, the effluent can still reduce its CO_2 content through an increase of bicarbonate because of unreacted carbonate mineral. This requires that the carbonate mineral is available in the plume near the unreacted solution.

If the EWL discharged its ionic effluent below the CCD as the EPWL does, no degassing and carbonate precipitation will occur, but the CO_2 dissolved in the ionic effluent (column c of Table 3-1) will be added to the seawater increasing the overall ocean acidity; in this case, the CO_2 storage efficiency is 100%, because all the CO_2 entered into EWL process does not return to the atmosphere. If, before sending the EWL effluent to a depth below the CCD, a degassing of the ionic solution is done (column d of Table 3-1), part of the CO_2 will return to the atmosphere, decreasing the overall storage efficiency and still leaving

unreacted CO_2 that will contribute to the ocean acidification (1,212 µmol/kg in point d of Table 3-1).

In the EPWL, the carbonate mineral's dissolution reaction will continue in the effluent plume until all the carbonate mineral is dissolved, and almost all the CO_2 is stored in bicarbonate form, without lowering the seawater pH.

The quantity of ionic solution that would be sent by a pipeline to a depth below the CCD with an EWL reactor corresponds to the needed amount of water for dissolving the carbonate mineral (point c of Table 3-1), or approx. 3,800 m_3 per tonne of CO_2, Table 3-1 (hypothesis of 150,000 µatm of pCO_2).

The quantity of water sent into the pipeline in the EPWL case depends only on the allowable pH at the release point, because almost the complete dissolution process of the carbonate mineral will occur in the plume. In the EPWL case study considered below, 500 m_3 per tonne of CO_2 stored are considered in the pipeline to release an effluent with a pH of 6.1. Therefore, the pipeline needed for "storing" the same quantity of CO_2 below the CCD could be much smaller in the EPWL case than in the EWL one, also avoiding the problem of increased ocean acidification, as discussed above.

The feasibility of the EPWL, below the CCD, is reserved to few places with very deep-sea near the coast. Among them, it is possible to mention: Japan, Chile, Peru, Puerto Rico, Cuba, Jamaica, Philippines, Russia (Kamchatka), USA (Aleutines), Indonesia, Taiwan. The first examples of the bathymetry near some of these locations are shown in Figure 5-7.

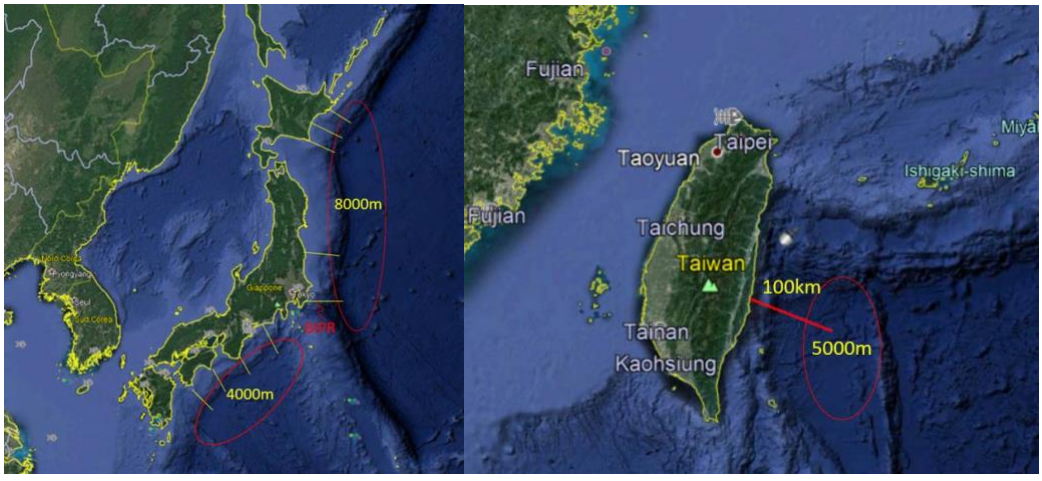

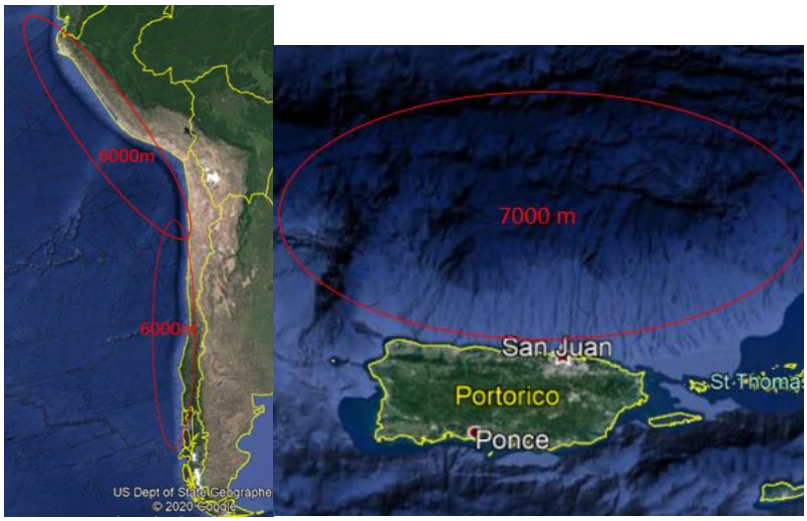

Figure 5-7: Bathymetry in some possible location of EPWL

5.7 EPWL – Discharge above the CCD (pHA-EPWL)

In places with lower sea depth like the Mediterranean Sea, where the CCD is never reached, the previous EPWL method could not be applied because a large quantity of water, similar to the one needed for the EWL technology, would be needed to dissolve all the carbonate mineral inside the pipeline before the discharge point.

Above the CCD, it is thus very important to dissolve all the carbonate mineral before the discharge point and to release all the Ca^{2+} in ionic form because above the CCD, the possible unreacted calcite ($CaCO_3$) could not be dissolved in the plume once it is released. It is worth noting that the other $CaCO_3$ form, aragonite, could dissolve above the CCD and below the Aragonite Compensation Depth (ACD). The ACD is the depth in the ocean at which the dissolution rate of aragonite is equal to the rate at which aragonite accumulates. In seawater, aragonite is less stable than calcite. Consequently, the ACD is shallower than CCD. The current depth of the ACD in the Atlantic Ocean ranges from 2,000 m to 3,000 m and in the Pacific and the Indian Ocean from 500 m to 1,500 m. Following the acidification of the seas caused by the increase of CO_2 in the atmosphere, the ACD is going to ever lower depths: in some waters, the ACD coincides with the sea's surface.

Another point to be considered is the risk of precipitation. In the current seawater, the Mg/Ca ratio is approximately 5.2. This implies that once calcium is in the ionic form Ca^{2+}, no precipitation of carbonate can occur as calcite, but only as aragonite. Above the ACD,

Ca^{2+} could precipitate as aragonite, thus the discharge should be avoided above the ACD, because the precipitation implies a release of CO_2 to the atmosphere.

5.7.1 Scheme of the technology

Two new configurations have then been studied to overcome the problem mentioned above of using a large amount of water to discharge an ionic solution into the sea between the ACD and the CCD, the pH Adjusted – Enhanced Pressurized Weathering of Limestone (pHA-EPWL): both adds to EPWL a floating reactor where a final carbonate mineral dissolution, then in one the pH adjustment is realized through a natural confined flow of seawater at first and secondly by an addition of calcium hydroxide. The latter buffers the remaining CO_2 to increase the final discharge's pH in the open waters and to guarantee complete CO_2 storage in the bicarbonate form. In the other configuration the complete dissolution of carbonate minerals is obtained by using a bigger floating reactor, and so considering an higher dissolution factor.

In both cases the first pipe, L-pipe (Limestone pipe), goes from the sea-level to 1,000 – 5,000 m depth, following the seabed, and it is used as a pressurized reactor for the dissolution of carbonate mineral with CO_2 and seawater. The floating mixer, called FS-MIX (Floating Submarine Mixer) is a tubular floating structure that goes from the bottom of the sea, where it is anchored, to a lower depth. Inside the FS-MIX, seawater is well mixed with the slurry discharged by the L-pipe at the top of the FS-MIX, for a proper residence time and dilution ratio. This configuration is shown in Figure 5-8-1.

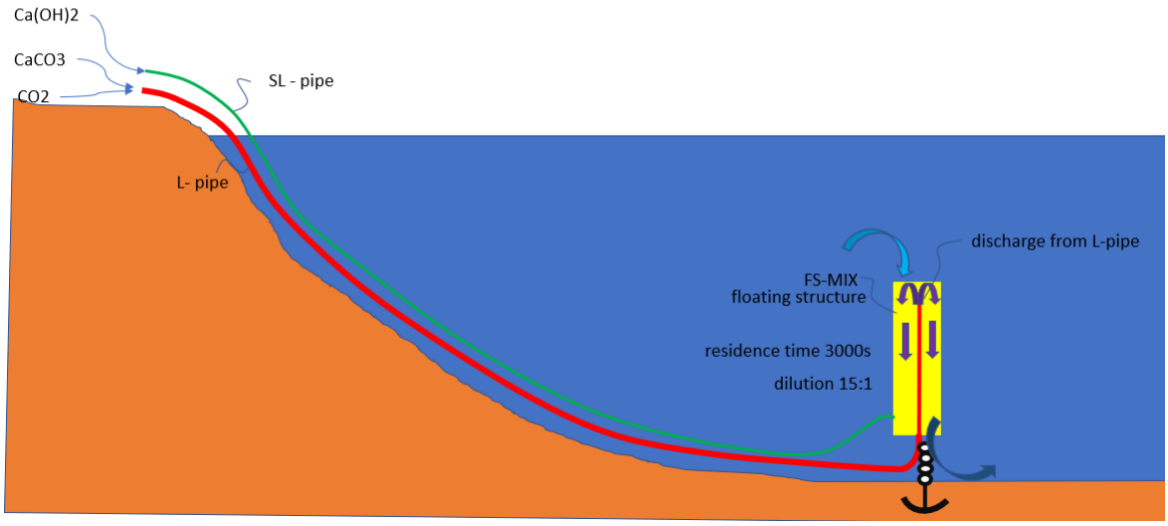

Figure 5-8-1: pHA-EPWL configuration (with calcium hydroxide)

In this first configuration the amount of carbonate minerals used at the beginning of the L-pipe is lower than the stoichiometric value, in order to accelerate the dissolution of it in seawater since there is an excess of CO_2 in it. The remaining CO_2 at the end of the FS-MIX reacts with the calcium hydroxide and is safely stored.

The reason for the FS-MIX is that, as said, at the L-pipe discharge point not all the carbonate mineral has reacted with the CO_2. The slurry discharged should be diluted with a proper quantity of seawater to finalize the carbonate mineral dissolution. The dilution of the slurry from the L-pipe could not be achieved in the natural plume generated by the slurry itself in free water at the discharge point because the dilution of the plume in the open sea is too high in a too short time to allow the dissolution of carbonate mineral to proceed.

The configuration without the calcium hydroxide has also been considered since the costs of the calcium hydroxide are high. In this new configuration, the FS-MIX diameter is higher and the dilution factor considered is 20:1, so 10,000 m_3 of seawater are needed to enter the floating reactor. The choice between one solution and the other is both technical and economical and it should be assessed case by case. The amount of carbonate minerals used is the stoichiometric one, in order to safely store all the CO_2. This second configuration is shown in Figure 5-8-2.

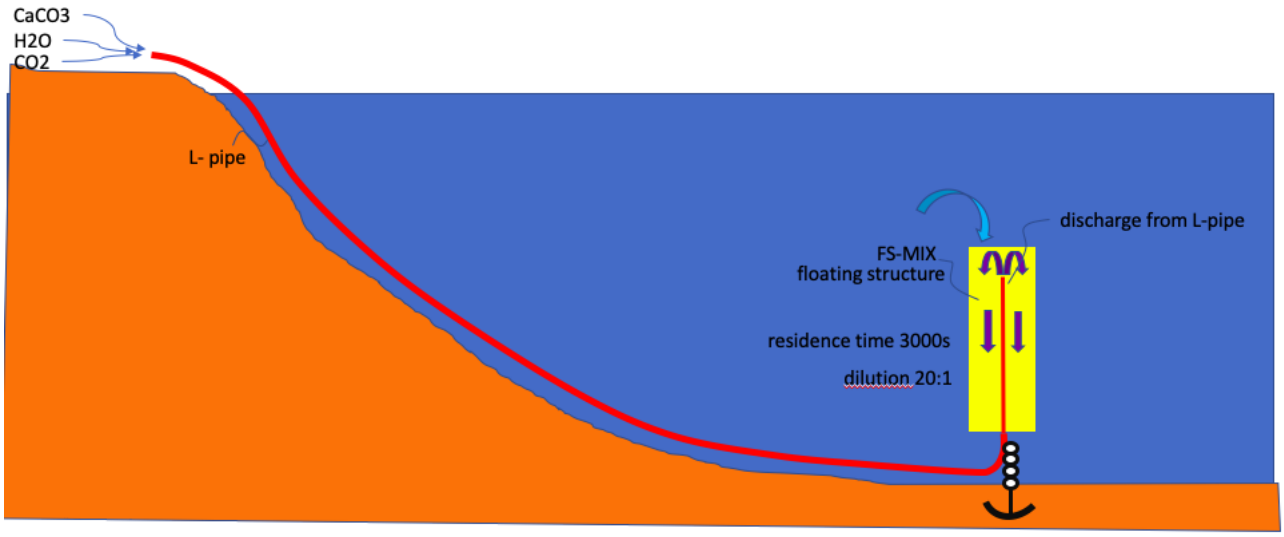

Figure 5-8-2: pHA-EPWL configuration (without calcium hydroxide)

Before considering the use of a confined plume, it was analyzed the possibility to dissolve the unreacted CaCO3 in an unconfined plume. The dilution factors' calculations have been done using the software Visual Plume 4th Edition (Frick et al., 2003). This computer

application simulates single and merging submerged plumes in arbitrarily stratified ambient flow and buoyant surface discharges.

In the simulations, it has been considered the solution that leaves the L pipe. Since it has amounts of unreacted $CaCO_3$ and CO_2, the solution is heavier than the surrounding seawater, and so it will sink. This calculation represents the condition of an unconfined plume in the ocean.

Figure 5-9 shows the dilution factor as a function of the horizontal distance from the discharge point. It is possible to understand from Figure 5-9 that this value is too high in the open sea in a too short time to achieve the full dissolution of the $CaCO_3$.

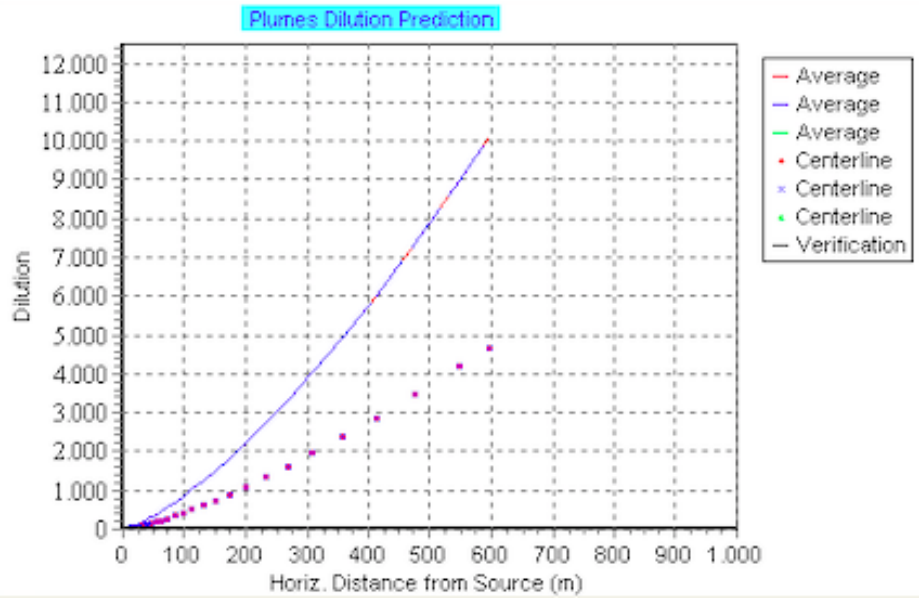

Figure 5-9: Dilution factor as a function of the horizontal distance from the source

A confined plume is needed to overcome this problem, where the dilution rate of the L-pipe effluent with the seawater could be carefully controlled along with the residence time, to guarantee the complete dissolution of the carbonate mineral. This controlled dilution in a confined plume could be realized through a second reactor, i.e., the FS-MIX.

5.7.2 Design of the FS-MIX

The FS-MIX could be a modular structure consisting of several pieces made of steel or plastic, anchored to the seabed and with floaters that allow the system to stay in a vertical position inside the deep ocean and to release part of the weight of the structure itself (Figures 5-10 and 5-11).

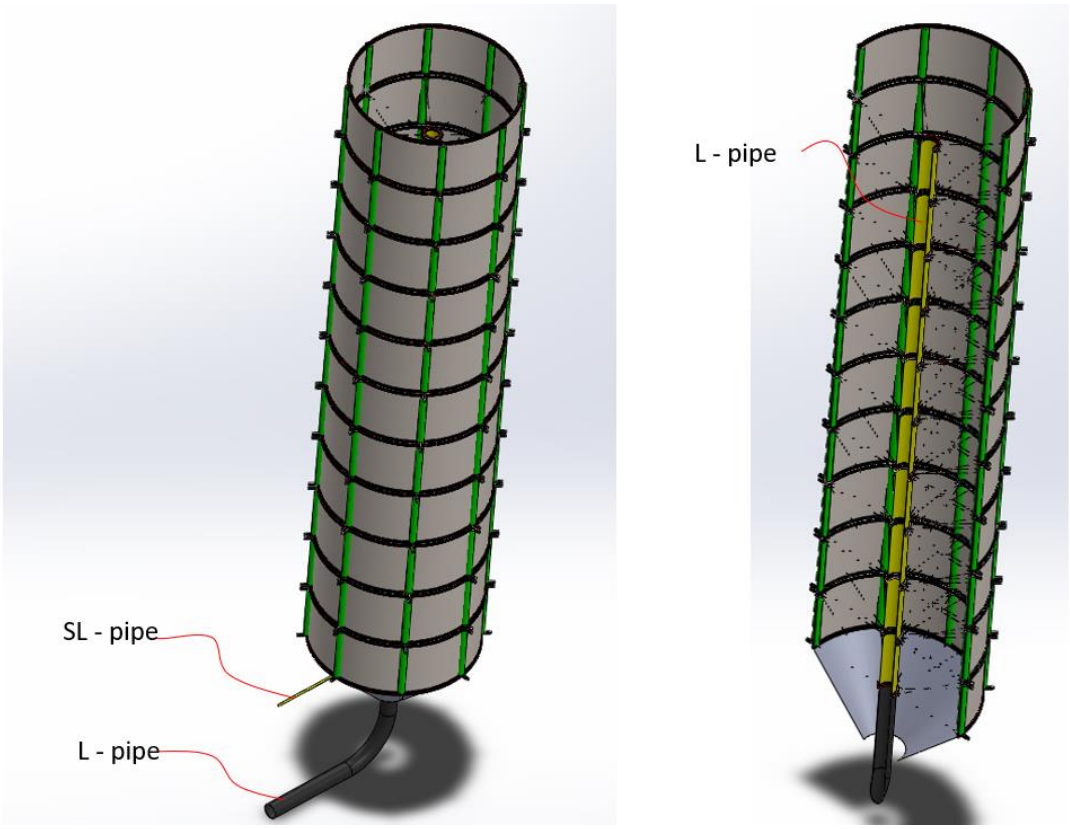

Figure 5-10: Configuration of the FS-MIX reactor

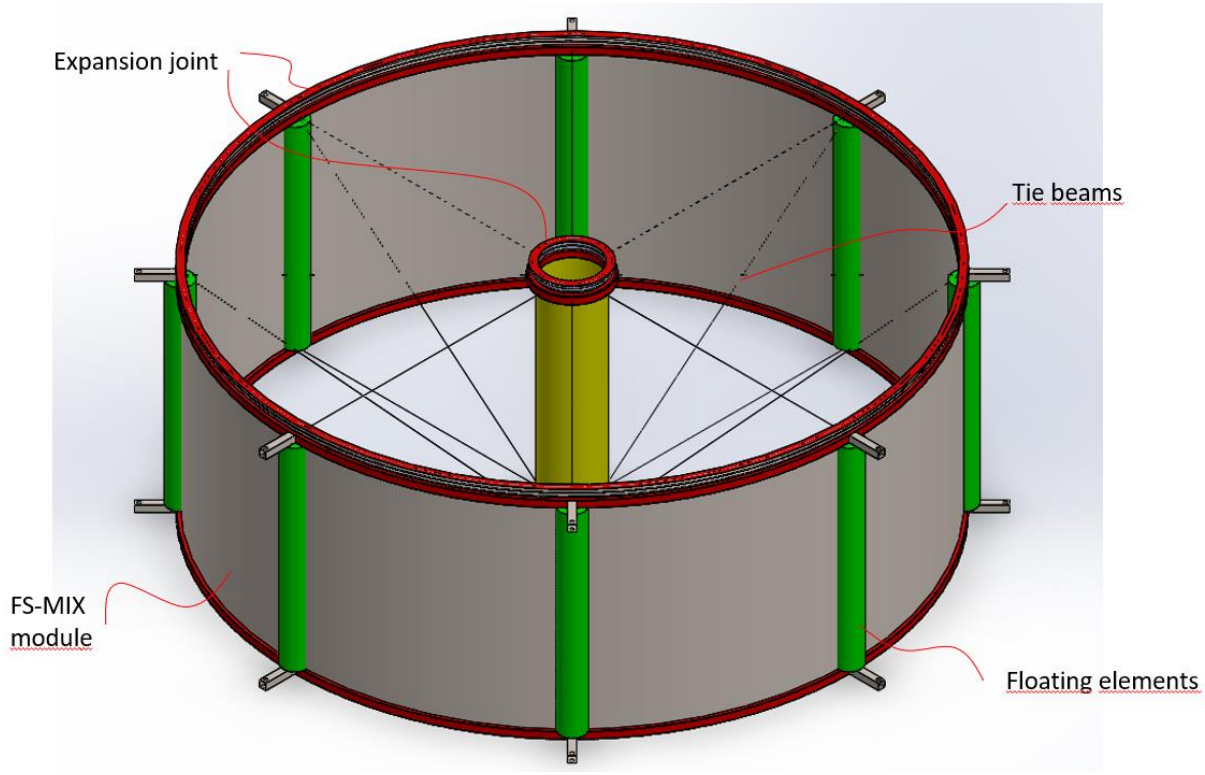

Figure 5-11: Module of the FS-MIX reactor

The FS-MIX could consist of either one big tubular structure or many smaller tubular structures working in parallel at the end of the L-pipe. For the aim of this study, only a single FS-MIX system will be considered.

The FS-MIX is a vertical tubular structure opened on both ends where the external seawater can enter from the top and the effluent-rich in bicarbonate discharged from the bottom.

The FS-MIX configuration should be studied and evaluated in detail in an engineering phase. Still, the idea is that the floating modules that compose the flexible structure will make any single module buoyant, so, once in place and anchored to the bottom of the sea, the FS-MIX will stay in an upward position. The structure has metallic Gimbal type (or similar) expansion joints to make it flexible and tight. A procedure for launching this kind of construction along with the HPDE pipes has been studied.

The acidic effluent from the L-pipe is heavier than the surrounding seawater. It will sink inside the FS-MIX, mixing with the fresh seawater entering from the top due to a light Venturi effect, forming a confined plume. The FS-MIX size could be calculated according to the dilution and residence time required for a complete dissolution of the carbonate mineral.

It seems convenient to use a sub-stoichiometric quantity of carbonate mineral compared with the one needed with Equation 3.3 to limit the FS-MIX dimensions. In this way, there is an excess of CO_2 both in the L-pipe and in the FS-MIX, accelerating the carbonate mineral dissolution reactions.

5.7.3 SL pipe

At the bottom of the FS-MIX, all the carbonate mineral will be completely dissolved, but a residual dissolved quantity of unreacted CO_2 is still present inside the effluent at the bottom of the FS-MIX because the initial quantity of carbonate mineral is sub-stoichiometric compared to the CO_2 injected in the L pipe.

To complete the reaction of this residual quantity of CO_2 and to compensate the lower pH of the effluent released by the FS-MIX compared to the seawater's one, calcium hydroxide is added at the lower part of the FS-MIX, before releasing the effluent to the sea.

A second pipe, called SL-pipe (Slacked Lime pipe), is thus considered to bring the proper quantity of calcium hydroxide for buffering the unreacted CO_2, allowing the effluent's discharge from the FS-MIX at the same pH of the surrounding seawater.

Even if a complete and detailed design of the process is needed to find the best working parameters, the numerical cases of Chapter 6.2 give results consistent with a practical engineering solution.

5.7.4 Assessment of the amount of water required (pHA-EPWL)

The amount of water in the L-pipe could be chosen according to economic or technical considerations: the fact that part of the dissolution reactions of the carbonate mineral is carried out in the FS-MIX and that the pH of the effluent could be controlled by using calcium hydroxide, gives a multiple variables problem, that will require more information to be solved.

The case analyzed in Chapter 6.2 is one of the possible solutions, but likely it is not the optimal one.

The quantity of water that will be sent into the pipeline in the pHA-EPWL case depends on the residence time and the FS-MIX's dilution factor, and, ultimately, on the FS-MIX size and cost.

The applicability of the PHA-EPWL, between the CCD and the ACD (Aragonite Compensation Depth), is possible on most of the coastlines where the sea is generally deeper of 2.000 m, because the pipe is 1,000 m long, within approximately 100 km from the coast. Among other places, the PHA-EPWL could be deployed in almost all the coasts of the Mediterranean sea, the Black Sea, Africa, Yemen, Oman and Pakistan, the East of India, Indonesia, Australia, USA, Brasil, Mexico.

For the Italian case, almost all the seas surrounding Italy except the Adriatic Sea are suitable for the PHA-EPWL technology.

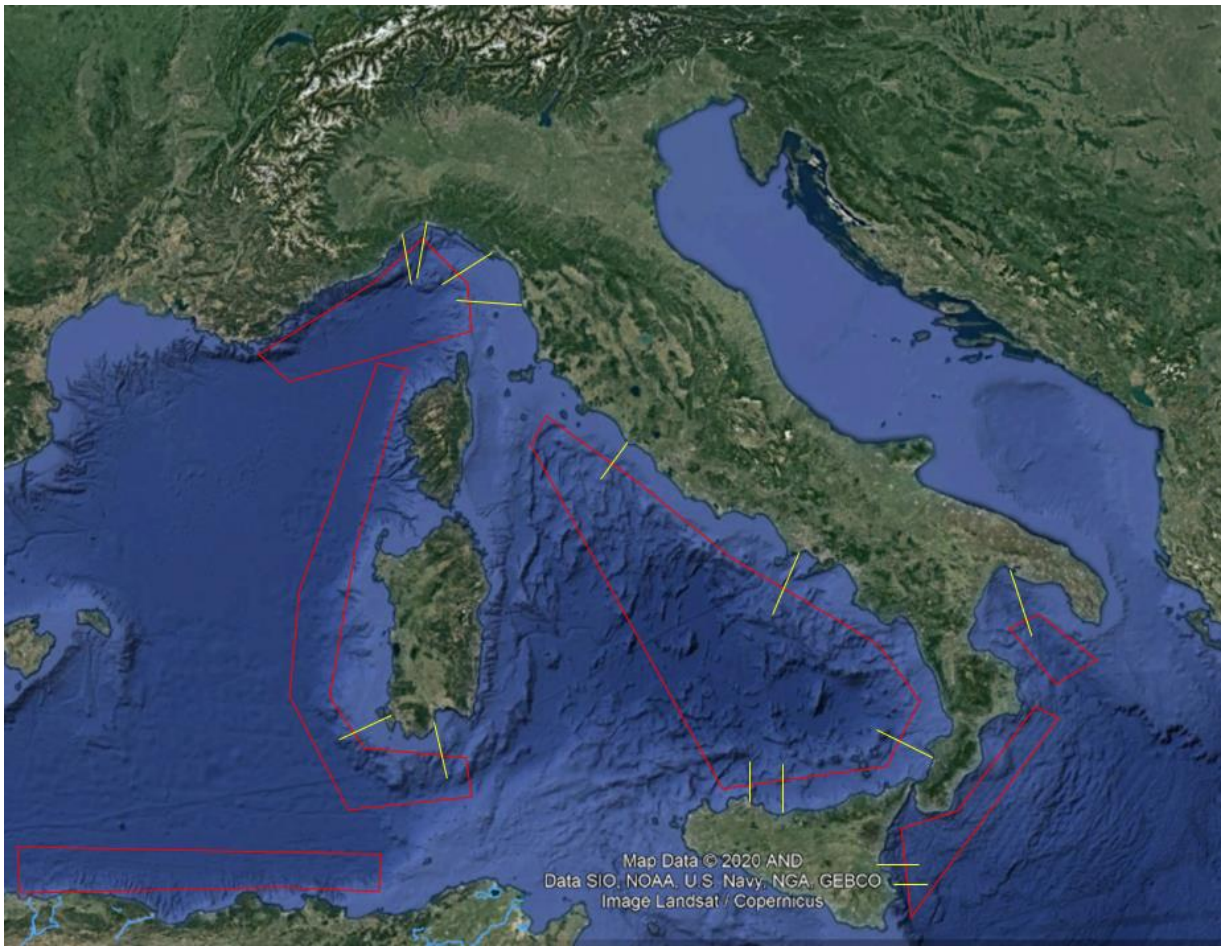

Figure 5-12: Bathymetry in some possible Italian location of pHA-EPWL

Chapter 6: CASE STUDY

6.1 EPWL case study: Tokyo

A case of a discharge in a deep-sea below the CCD considers a plant located near Tokyo (Figure 6-1). A pipe of 100 km, which follows the seabed down to 5,000 m, is considered to store 1,000 kg of CO_2. In the L- pipe, the stoichiometric quantity needed is 2,270 kg of carbonate mineral and 500 m_3 of seawater.

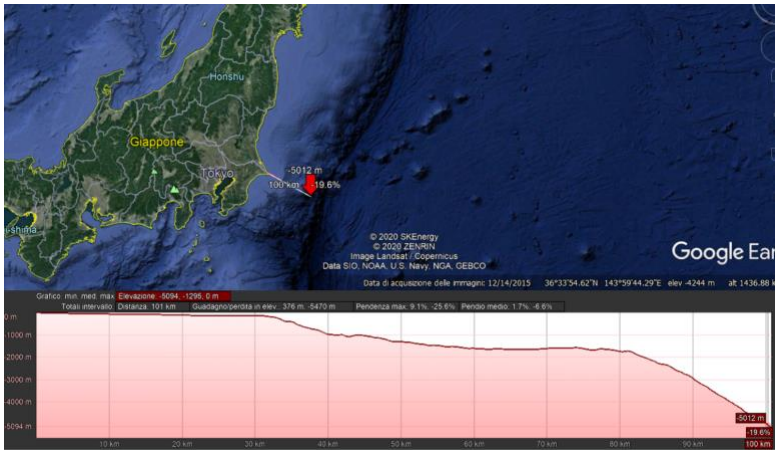

Figure 6-1: Tokyo case EPWL

Using the software PHREEQC, it has been calculated that at the discharge point of this pipe, there are still 1,100 kg of carbonate mineral and 617 kg of CO_2 unreacted, and the pH of the effluent is ~ 6.1.

The carbonate mineral used at the beginning of the L-pipe has a particle size of 50 µm, and has been calculated that this value becomes 34 µm at the discharge point of the L-pipe.

The effluent from the L-Pipe will form a descending plume into the deep sea because of the higher density of the effluent itself. With the software PHREEQC it is possible to evaluate that with the dilution of the effluent in the plume of 15 times, all the residual carbonate mineral will be dissolved and all the residual CO_2 will be stored in the form of HCO_3^-.

The system's final efficiency is 100 % because there will be no degassing of CO_2 and no precipitation of carbonate. The EPWL simplified mass balance is shown in Figure 6-2.

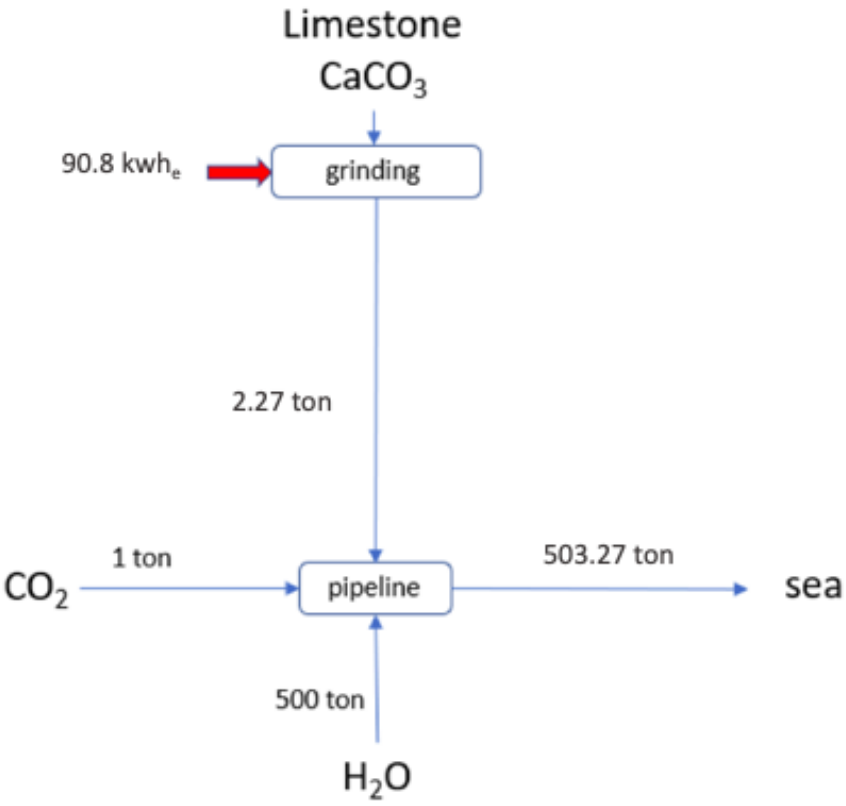

Figure 6-2: Mass and Energy balance of the EPWL

The energy needed for pumping water could be low (and it is not considered in this analysis) because its higher density and Δh promotes the flow of water, CO_2 and carbonate minerals inside the L-pipe compared to the surrounding seawater and by the descent of the L-pipe from the sea level to a depth of 5.000 m. The velocity of the water inside the L-pipe should be kept at approximately 1 m/s to avoid the particle deposition inside the L-pipe and to lower high pressure drops. The critical parameters of the EPWL in the considered case are shown in Table 6-1.

Table 6-1: Working parameters for the EPWL method

EPWL	Initial seawater (A)	In equilibrium with CO_2 (B)	In equilibrium with CO_2 and $CaCO_3$ (C)	Diluted with seawater (D)
pCO_2 (bar)		1.1	1.1	
$\sum$Alk ($\propto$eq kg^{-1})	2791	2791	15620	5803
$\sum CO_2$ ($\propto$mol kg^{-1})	2758	50000	16370	5902
$CO_{2(aq)}$ ($\propto$mol kg^{-1})	40	47200	844	166
HCO_3 ($\propto$mol kg^{-1})	2019	2143	10130	4005
CO_3^{2-} ($\propto$mol kg^{-1})	18	0.01	20	16
Ca^{2+} ($\propto$mol kg^{-1})	9018	9025	14870	10460
SI_{cal}	0.35	-2.67	-0.07	-0.08
pH	8	4.952	6.993	7.434

6.1.1 Preliminary cost assessment Tokyo EPWL

A preliminary cost assessment of the EPWL configuration is presented in this chapter. A module for storing 250,000 tonne/year of CO_2 working 8,000 h/year is considered. The key parameters are reported in Table 6-2.

Table 6-2: Main parameters (EPWL)

	Unit	**Quantity**
CO_2	kg/s	9.53
Carbonate mineral	kg/s	21.63
Water	kg/s	4,765.00
Depth	m	5,000

The CO_2 is provided to the EPWL at a 1.1 bar to guarantee the complete dissolution of it in the seawater, while the limestone is provided at the plant with a maximum dimension of 500 mm. The carbonate mineral is extracted from the quarry in blocks of 500 mm and grinded to 50 μm: the electrical consumption of this operation is 40 kWh/tonne$_{CaCO3}$ (Clirik,2020).

A minimum velocity is needed inside the pipe to avoid the particle deposition inside the L-pipe. Considering the L-pipe diameter of 2.4 m, the velocity is 0.96 m/s, enough to avoid this problem.

The amount of seawater used is 500 m^3 per tonne of CO_2, so the L-pipe flow is 3.4 m^3/s. Using the site Pressure Drop Online Calculator, the pressure drop has been evaluated in these conditions, and the result is 1.5 bar of pressure loss (Pressure Drop Online-Calculator,2020).

There is an amount of energy given by the weights of the CO_2 and the $CaCO_3$, that result in energy saved pumping.

The pump data are listed in Table 6-3, reaching a final consumption of 14.99 $kWh/tonne_{CO2}$.

Table 6-3: Pump parameters (EPWL)

	Unit	**Quantity**
Discharge depth	m	1,500
Potential energy	kJ	1,379,531.25
Energy saved pumping	kWh	383.20
Pressure loss	bar	1.5
Efficiency	%	75
Pumping	kWh	851.56
Specific consumption	$kWh/tonne_{CO2}$	14.99

The main parameters of the L-pipe are then shown in Table 6-4.

Table 6-4:L-pipe parameters (EPWL)

	Unit	**Quantity**
Length	m	70,000
Diameter	mm	2,400
Installation	€/km	200,000
Pipeline weigth HDPE	kg/m	521.50
HDPE polymer	€/kg	1
Electric extrusion energy	MWh/t	0.75
Electric energy	€/MWh	50
Total cost HPDE pipeline	€	36,168,909
Electric energy extrusion	€	1,356,334
Industrial margin	%	25
Total cost pipeline	€	46,906,554
Installation pipeline	€	14,000,000
TOTAL COST	€	60,906,554

Considering a lifetime of 100 years for the structure, it is possible to calculate the CAPEX costs/tonneCO_2.

Table 6-5: CAPEX cost (EPWL)

	Unit	**Quantity**
Total L-pipe	€	60,906,554
Total mills limestone	€	10,000,000
Others (pumps,electric cabinets, civil)	€	5,000,000
TOTAL CAPEX	€	75,906,554
Lifetime plant	years	100
Total CO_2 lifetime	ton	25,000,000
CAPEX COST	€/tonne	3.0

The specific CAPEX cost of the EPWL is then 3 €/tonneCO_2 stored.

The raw materials need to be crushed to a particle size of 50 μm to dissolve all the carbonate minerals. This process requires electricity and this is considered in the OPEX

costs, together with the transportation of the minerals with ships. This cost is not fixed because it depends on the carbonate minerals' value, then a maximum and minimum price has been evaluated.
The production cost of limestone varies between 2.5-7.5 €/tonne, and also considering the transportation costs, the final price is between 5.25-10.25 €/tonne (Clirik, 2020)

The crushing of limestone requires 40 kWh/tonne$_{CaCO3}$, and by considering a cost for the electricity of 40 €/kWh, the total cost for grinding the carbonate minerals is 4.54 €/tonne$_{CO2}$ (Clirik, 2020)

The OPEX cost for the EPWL is reported in Table 6-6.

Table 6-6: OPEX cost (EPWL)

	Unit	**Minimum Quantity**	**Maximum quantity**
Limestone	€/tonne$_{CO2}$	5.25	10.25
Electricity	€/tonne$_{CO2}$	4.54	4.54
Others(peronnel,etc.)	€/tonne$_{CO2}$	5	5
TOTAL COST	€/tonne$_{CO2}$	14.79	19.79

According to this preliminary evaluation, the total cost of the EPWL storage varies between 17.79-22.79 €/tonne$_{CO2}$ stored, considering an industrial margin of 50%, the final storage cost is 26.685-34.185 €/tonne$_{CO2}$ stored.
This cost could vary depending mainly on the limestone and energy cost.

6.2 pHA-EPWL case study: Genova

6.2.1 Configuration with the calcium hydroxide

A case of discharge above the CCD considers a plant located in Genova (Figure 6-3). A pipe of 70 km, which follows the seabed up to 2,500 m, is considered to store 1,000 kg of CO_2, using 2,000 kg of carbonate mineral and 500 m^3 of seawater. The quantity of carbonate mineral used in the L- pipe is less than the stoichiometric amount needed of 2,270 kg because part of the buffering is done later in the FS-MIX by the calcium hydroxide.

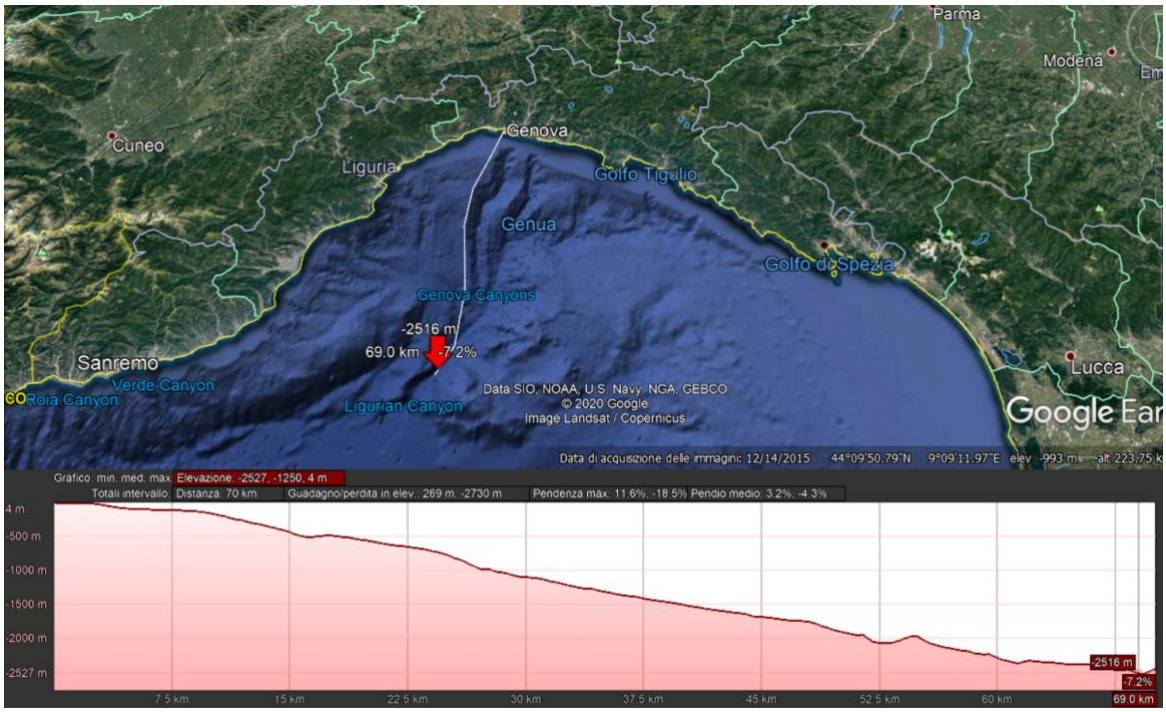

Figure 6-3: Genova case pHA-EPWL

Using the software PHREEQC it has been calculated that at the discharge point of this pipe, there are still 1,066 kg of unreacted carbonate mineral and 632 kg of unreacted CO_2, and the pH of the effluent is ~ 6.1. The first step is to calculate the effluent's characteristics that leave the L-pipe and enter the FS-MIX. The carbonate mineral used at the beginning of the L-pipe has a particle size of 50 µm, and it has been calculated that at the discharge point of the L-pipe, this value becomes 34 µm.

This effluent enters the upper part of the FS-MIX, at 1,000 m above the seabed. Inside it, the effluent is diluted with 7,500 m_3 of seawater, which enters naturally in the FS-MIX since the effluent that leaves the L pipe is heavier than the surrounding seawater so that it will sink.

Using the software PHREEQC, it has been evaluated that all the carbonate mineral has reacted when seawater reaches the bottom of the FS-MIX, while about 130 kg of CO_2 are still dissolved in the water (pH=7.2).

To safely store this remaining CO_2 and to discharge the water with a pH similar to the seawater one, calcium hydroxide is added to the effluent at the bottom of the FS-MIX.

According to the PHREEQC results, 3 k-moles of CO_2 are buffered by almost 2 k-moles of $Ca(OH)_2$, thus 150 kg of $Ca(OH)_2$ are needed to buffer 130 kgCO_2. Calcium hydroxide is dissolved in 50,000 kilograms of seawater and pumped in the lower part of the FS-MIX through the SL-pipe. In this way all the carbon dioxide has reacted inside the FS-MIX and the effluent is discharged from the FS-MIX at pH is 8.024, close to the seawater one of 8.
The system's final efficiency is lower than 100 % because some of the CO_2 stored is produced in the calcination process. If the calcination is performed by an electric calcinator and all the resulting CO_2 is sent to the storage system and all the electric energy required by the system is renewable, the following simplified mass balance could be the one shown in Figure 6-4.

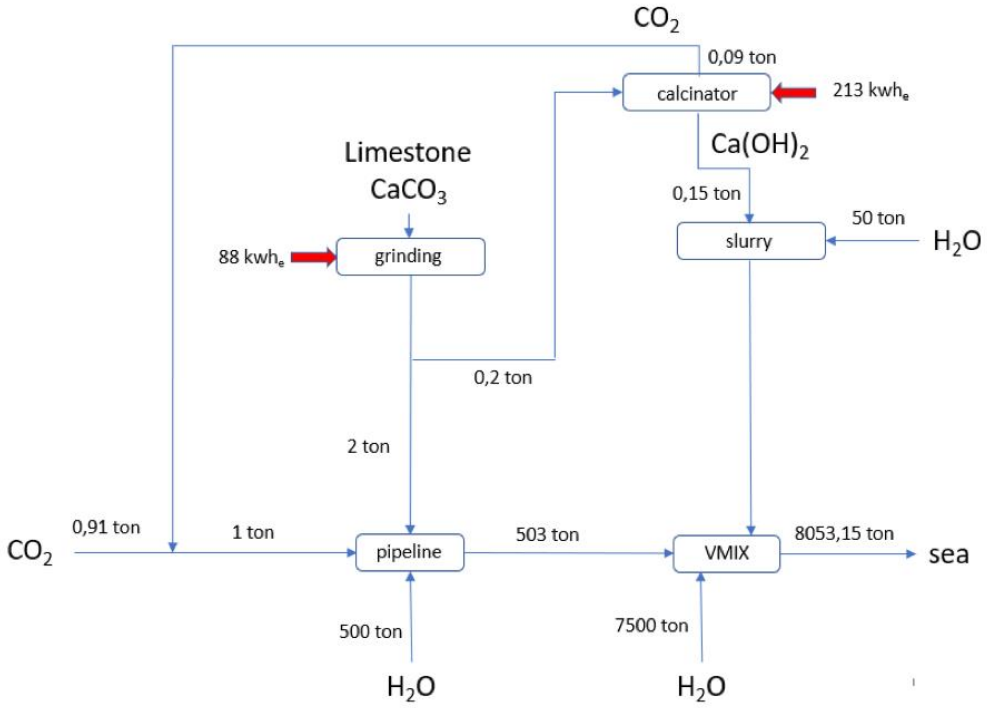

Figure 6-4: Mass and Energy balance of the process of the pHA-EPWL (with calcium hydroxide)

The energy needed for pumping water is low (and it is not considered in this analysis) because the flow of water, CO_2 and carbonate inside the L-pipe is promoted by both its higher density compared to the surrounding seawater and by the descent of the L-pipe from the sea level to a depth of 1500 m (the upper part of the FS-MIX).
In this way, 1 tonne of CO_2 can be stored with an efficiency of 91%, through the use of 2 tonne of carbonate mineral, 0.15 tonne of $Ca(OH)_2$ and 500 tonne of seawater added into the L pipeline and 7,500 tonne of seawater naturally flowing in the FS-MIX. The pH at the discharging point of the FS-MIX is almost equal to the seawater one.

The critical parameters of the pHA-EPWL in the considered case are shown in Table 6-7.

Table 6-7: Working parameters for the pHA-EPWL method (with calcium hydroxide)

EPWL-pHA (with calcium hydroxide)	Initial seawater (A)	In equilibrium with CO_2 (B)	End of L-pipe (C)	After dilution and at the end of VMIX (D)	In equilibrium with $Ca(OH)_2$ (E)
pCO_2 (bar)		1.1	1.1		
∑Alk (∝eq kg^{-1})	2791	2791	45320	5510	6023
∑CO_2 (∝mol kg^{-1})	2758	50000	71340	5879	5858
$CO_{2(aq)}$(∝mol kg^{-1})	40	47200	26040	397	54
HCO_3 (∝mol kg^{-1})	2019	2143	31900	3995	4094
CO_3^{2-} (∝mol kg^{-1})	18	0.01	6	7	54
Ca^{2+} (∝mol kg^{-1})	9018	9025	27120	10280	10490
SI_{cal}	0.35	-2.67	-0.02	-0.29	0.61
pH	8	4.952	6.161	7.151	8.027

It is possible to see that almost all the CO_2 is finally stored as HCO_3^-.

6.2.2 Configuration without the calcium hydroxide

The same case of Chapter 6.2.1 is considered for the configuration of pHA-EPWL without the SL-pipe. A pipe of 70 km, which follows the seabed up to 2,500 m, is considered to store 1,000 kg of CO_2, using 2,270 kg of carbonate mineral, the stoichiometric value, and 500 m^3 of seawater.

Using the software PHREEQC it has been calculated that at the discharge point of this pipe, there are still 1,261 kg of unreacted carbonate mineral and 688 kg of unreacted CO_2, and the pH of the effluent is ~ 6.1. The first step is to calculate the effluent's characteristics that leave the L-pipe and enter the FS-MIX. The carbonate mineral used at the beginning of the L-pipe has a particle size of 50 µm, and it has been calculated that at the discharge point of the L-pipe, this value becomes 35 µm.

This effluent enters the upper part of the FS-MIX, at 1,000 m above the seabed. Inside it, the effluent is diluted with 10,000 m^3 of seawater, which enters naturally in the FS-MIX since the effluent that leaves the L pipe is heavier than the surrounding seawater so that it will sink.

The system's final efficiency is 100 % because there will be no degassing of CO_2 and no precipitation of carbonate. The EPWL simplified mass balance is shown in Figure 6-5.

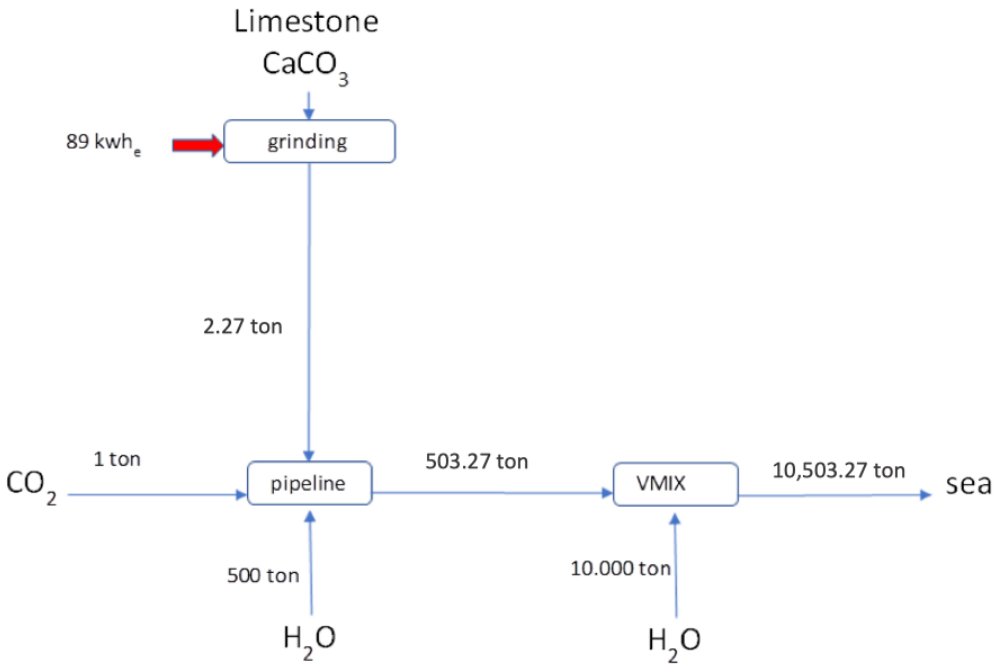

Figure 6-5: Mass and energy balance of the pHA-EPWL (without the calcium hydroxide)

In Table 6-8 are listed the key parameters of the technology.

Table 6-8: Working parameters for the pHA-EPWL method (without calcium hydroxide)

EPWL-pHA (witohut calcium hydrxide)	Initial seawater (A)	In equilibrium with CO_2 (B)	End of L-pipe (C)	After dilution and at the end of VMIX (D)
pCO_2 (bar)		1.1		
∑Alk (∝eq kg^{-1})	2791	2791	43070	4899
∑CO_2 (∝mol kg^{-1})	2758	50000	74360	5041
$CO_{2(aq)}$(∝mol kg^{-1})	40	47200	31290	188
HCO_3 (∝mol kg^{-1})	2019	2143	31150	3522
CO_3^{2-} (∝mol kg^{-1})	18	0.01	5	7.5
Ca^{2+} (∝mol kg^{-1})	9018	9025	26120	10140
Si_{cal}	0.35	-2.67	0	-0.26
pH	8	4.952	6.142	7.213

6.2.3 Preliminary cost assessment Genova pHA-EPWL

A preliminary cost assessment of the pHA-EPWL configuration is presented in this chapter.

A module for storing 250,000 tonne/year of CO_2 working 8,000 h/year is considered.

The key parameters are reported in Table 6-9

Table 6-9: Main parameters (pHA-EPWL)

	Unit	**Quantity**
CO_2	kg/s	9.53
Carbonate mineral	kg/s	21.63
Water	kg/s	4,765.00
Depth	m	5,000

The L-pipe data and the pump data are the same as the EPWL case, while in this case the FS-MIX cost needs to be added to the CAPEX costs.

The main parameters of the FS-MIX are reported in Table 6-10.

Table 6-10:FS-MIX parameters (pHA-EPWL with calcium hydroxide)

	Unit	**Quantity**
Diameter	m	15.77
Flow	m^3/s	65.10
Velocity	m/s	0.33
Length	m	1000
Residence time	s	3000
Weight steel FS-MIX	tonne	6,000
Specific steel cost HY 80	€/tonne	1,000
Total cost steel FS-MIX	€	6,000,000
Industrial margin	%	50
Total cost FS-MIX	€	9,000,000
Installation cost	€	5,000,000
TOTAL COST	€	14,000,000

Considering a lifetime of 100 years for the structure, it is possible to calculate the CAPEX costs/tonne$_{CO2}$.

Table 6-11: CAPEX cost (pHA-EPWL with calcium hydroxide)

	Unit	**Quantity**
Total L-pipe	€	74,906,554
Total mills limestone	€	10,000,000
Others (pumps,electric cabinets, civil)	€	5,000,000
TOTAL CAPEX	€	89,906,554
Lifetime plant	years	100
Total CO_2 lifetime	ton	25,000,000
CAPEX COST	€/tonne	3.6

The specific CAPEX cost of the pHA-EPWL is then 3.6 €/tonne$_{CO2}$ stored.

The considerations regarding the grinding and the transportation of the carbonate mineral are the same as the EPWL, so their cost is reported in Table 6-6. In the specific OPEX cost of the pHA-EPWL needs to be also considered the electric calcinatory.
The calcination is done using an electric calcinator, and in this way, all the CO_2 is stored. This process requires a lot of energy, 213 kWh/tonne$_{CO2}$, and by considering the same cost of electricity as before, the added value of this process is 24.17 €/tonne$_{CO2}$.
According to this very preliminary evaluation, the total cost of the pHA-EPWL storage varies between 42.56-47.56 €/tonne$_{CO2}$ stored, considering an industrial margin of 50%, the final storage cost is 63.84-71.34 €/tonne$_{CO2}$ stored.
This cost could vary depending mainly on the limestone and energy cost.
The costs are higher with respect to the EPWL, but half of them are related to the calcination process. Thus, in the further study, the system will be considered without the electric calcinator, but using a higher dilution factor to dissolve all the reactants before the end of the FS-MIX.

Another configuration for the pHA-EPWL has then been considered, without the electric calcinator, but considering a higher dilution factor.
Instead of 7,500 m^3 of seawater inside the FS-MIX are required 10,000 m^3, so the floating reactor has to be bigger.

Table 6-12: Main parameters FS-MIS (pHA-EPWL without calcium hydroxide)

	Unit	**Quantity**
Diameter	m	18.21
Flow	m^3/s	86.81
Velocity	m/s	0.33
Length	m	1000
Residence time	s	3000
Weight steel FS-MIX	tonne	6,000
Specific steel cost HY 80	€/tonne	1,000
Total cost steel FS-MIX	€	6,000,000
Industrial margin	%	50
Total cost FS-MIX	€	9,000,000
Installation cost	€	5,000,000
TOTAL COST	€	14,000,000

Since the FS-MIX costs are lower than the L-pipe ones, the final specific CAPEX cost is the same, but the OPEX cost is lower.

According to this very preliminary evaluation, the total cost of this configuration of the pHA-EPWL storage varies between 18.39-23.39 €/tonne$_{CO2}$ stored, considering an industrial margin of 50%, the final storage cost is 27.58-35.08 €/tonne$_{CO2}$ stored.

From this very preliminary assessment it seems that it is more convenient to increase the size of the FS-Mix instead having a smaller FS-MIX with final addition of hydroxide.

Chapter 7: Conclusions

This study aims to evaluate the feasibility of EPWL as a technology for CO_2 storage. The results obtained show that this method is competitive with respect to the other, more developed CO_2 storage technologies. In particular, EPWL represents an alternative for emissions sources located in coastal areas where CO_2 injection in geological formations is not an option for storing the large amount of CO_2 emitted, and where the logistic cost of transporting the CO_2 to a geological storage are too high, to pursue ambitious global temperature stabilization targets.

In Table 7-1 are presented the main parameters of the 3 EPWL configuration calculated in this study, together with the EWL ones.

Table 7-1: Key parameters of the various technologies

	EWL	**EPWL**	**pHA-EPWL (with calcium hydroxide)**	**pHA-EPQL (without calcium hidroxide)**
Pumped Water (m^3)	3,800	500	500	500
Water flowing by gravity (m^3)	-	-	7,500	10,000
pH after dilution in seawater	7.1	7.5	8	7.7
Depth of discharge	Surface	Below the CCD (i.e. 4,000-5,000 m)	Above the CCD	Above the CCD
Carbonate mineral (kg)	2,270	2,270	2,000 (+ 270 in the calcinator)	2,270
Cost ($/ton$_{CO2\ stored}$)	18-128	26-34	63-71	27-35

The EPWL has clear advantages over the EWL technology:

- the amount of water needed for the process is lower, considering the same initial amounts of CO_2 and carbonate minerals;
- the risk that the carbonate precipitates is null since the discharge is below the CCD in EWPL and in pHA-EPWL the complete dissolution is obtained before the discharge point from the FS-MIX;

- all the unreacted CO_2 inside the pipe in the EPWL will react in the plume with the carbonate mineral to form bicarbonates;
- the risk of CO_2 degassing is null;
- there is no addition of acidity to the ocean even in a temporary basis.

Furthermore, the EWL needs a final degassing done in the sea to eliminate the effluent's residual acidity: this degassing is a long process that can take place only if the discharge point is in shallow water. This means that if the effluent from the EWL is discharged into the deep sea, it will never degas, leading to the seawater's permanent acidification.

The EPWL and the pHA-EPWL are not suitable for shallow water above the ACD, where they will face the same problems of degassing and carbonate precipitation of the EWL.

Using the pHA-EPWL it is possible to reach a final pH similar to the initial seawater, not affecting the marine environment. The use of an addition of calcium hydroxide allow to reduce the size of the FS-MIX; this means less materials and installation costs, and a smaller structure is less subjected to the influence of the currents present in the sea.
The main problem of the configuration without the calcium hydroxide is the high specific cost of calcium hydroxide production, since an electric calcinator has been considered. In the configuration of pHA-EPWL without the calcium hydroxide, on the contrary, the costs are lower, close to the EPWL case, but a bigger FS-MIX is needed, and also the pH at the discharge point is lower compared to the initial seawater's one.

The EPWL has several advantages also compared to the geological storage:
it is modular;

- the specific CAPEX cost is lower;
- it can be manufactured in a standardized form and deployed in a scheduled way;
- most countries have suitable coastlines and sea depths;
- it requires shorter and easier preliminary studies;
- the duration of the storage site depends on the materials lifetime and not on the saturation of a reservoir;
- there is no need of monitoring the area after the closure of the storage factory;
- the risk of leakage of the CO_2 from the storage is absent;

- there is the possibility to be also implemented from any port cities with suitable sea conditions;
- the CO_2 is managed at low-pressure.

A relevant benefit of this method is that EPWL and pHA-EPWL-derived water are characterized by elevated alkalinity. Their discharge into the marine environment enhances the oceanic buffer capacity and counteract the ongoing acidification due to the high concentrations of CO_2 in the atmosphere (Kirchner et al., 2020). This is of great importance for marine organisms and to face the “evil twin of global warming”, as ocean identification has been called.

There are also cons of the EPWL and the pHA-EPWL compared to the geological storage:

- high consumption of limestone and higher consumption of electricity, if no considering the compression of the CO_2;
- several countries do not have suitable coastlines and sea depths;
- there could be the impact (to be evaluated) for the marine environment of impurities present in the limestone;
- the storage cost is competitive for small emission sources, but probably higher than the storage cost for large CCS storage plant.

Further research is needed to assess this technology's feasibility as a largescale storage option, as well as the related political, social, and environmental challenges, related mainly to the mining of large amounts of limestone. Also, a more accurate cost analysis needs to be done, along with a life cycle assessment in order to evaluate the overall benefits and cost of this technology.

References

Adams, E., Caldeira, K. (2008). Ocean Storage of CO_2. *Elements, 4*, 319-324.

Adams, E., Golomb, D., Herzog, H. (1995). Ocean disposal of CO_2 at intermediate depth. *Energy Convers, 36*(6-9), 447-452.

Agudo, E., Kowacz, M., Putnis, C., Putnis, A. (2010). The role of bckground electrolytes on the kinetics and mechanism of calcite dissolution. *Geochimica et Cosmochimica, 74*, 1256-1267.

Ajayi, T., Gomes, J., Bera, A. (2019). A review of CO_2 storage in geological formations emphasizing modeling, monitoring and capacity estimation approaches. *Petroleum Science, 16*, 1028-1063.

Blunt, M. (2010). Carbon dioxide storage. *Imperial college London.*

Bui, M., Adjiman, C., Bardow, et al. (2018). *Carbon capture and storage (CCS): the way forward.* Energy & Environmental Science.

Burton, M., Bryant, S. (2009). Eliminating Buoyant Migration of Sequestered CO_2 Through Surface Dissolution: Implementation Costs and Technical Challenges. *SPE REservoir EValuation & Engineering*.

Bustos-Serrano, H., Morse, J. W., Millero, F. J. (2009). The formation of whitings on the Little Bahama Bank. *Marine Chemistry, 113*, 1-8.

Buttinelli, M., Procesi, M., Cantucci, B., et al. (2011). The geo-database of caprock quality and deep saline aquifers distribution for geological storage of CO_2 in Italy. *Energy, 36*, 2968-2983.

Caldeira, K., Rau, G. (2000). Accelerating carbonate dissolution to sequester carbon dioxide in the ocean: Geochemical implications. *Geophysical Research Letters, 27*(2), 225-228.

Campo, F., Caserini, S., Pagano, D., et al. (2020). Life cycle assessment of a process to remove atmospheric CO_2 and contrast ocean acidification. *Ingegneria dell'Ambiente, 7*.

Carbon Capture Journal. (2019). CO2-DISSOLVED: combining CO_2 geological storage with geothermal heat recovery.

Caserini, S., Dolci, G., Azzellino, A., et al. (2017). Evaluation of a new technology for carbon dioxide submarine storage in glass capsules. *International Journal of Greenhouse Gas Control, 60*, 140-155.

Chen, B., Song, Y., Nishio, M., et al. (2005). Modelling near-field dispersiojn from direct injection of carbon dioxide into the ocean. *Journal of geophysical research, 110*.

Clirik . (2020, 9 1). Retrieved from https://m.clirikchina.com

de Moel, P., van der Helm, A., van Rijn, M., van Dijk, J., & van der Meer , W. (2013). Assessment of calculation methods for calcium carbonate saturation in drinking water for DIN 38404-10 compliance. *Drinking Water Engineering and Science, 6*, 115-124.

Eke, P., Haszeldine, S., Naylor, M., Curtis, A. (2011). CO2/Brine Surface Dissolution and Injection: CO_2 Storage Enhancement . *SPE Projects,FAcilities & Construction*.

Esene, C., Rezaei, N., Aborig, A., Zendehboudi, S. (2019). Comprehensive review of carbonated water injection for enhanced oil recovery. *Fuel, 237*, 1086-1107.

Frick, W., Roberts, P., Davis, L., Keyes, J., Baumgartner, D., & George, K. (2003). *Dilution Models for Elffuent Dischaerges.* Ecosystem Research Division.

Giles, D., Ritchie, I., Xu, B. (1993). The kinetics of slaked lime. *Hydrometallurgy, 32*, 119-128.

Gledhill, D., Morse, J. (2006). Calcite dissolution kinetics in Na-Ca-Mg-Cl brines. *Geochimica et Cosmochimica, 70*, 5802-5813.

Global CCS Institute. (2019). *Global Status of CCS.*

Golomb, D., Pennell, S., Ryan, D., Barry, E., & Swett, P. (2007). Ocean Sequestration of Carbon Dioxide: Modelling the Deep Ocean Release of a Dense Emulsion of Liquid CO2-in-water Stabilized by Pulverized Limestone Particles. *Environmental Science & Technology, 41*, 4698-4704.

Gruber, J., & Sarmiento, N. (2006). *Ocean Biogeochemical Dynamics.* Princeton University Press.

Gunnarsson , I., Aradottir, E., Oelkers, E., et al. (2018). The rapid and cost-effective capture and subsurface mineral storage of carbon and sulfur at the CarbFix2 site. *Internatuonal Journal of Greenhouse Gas Control, 79*, 117-126.

Hansen, J., Sato, M., Kharecha, P., et al. (2008). Target Atmospheric CO2: There Should Humanity Aim?

Hasanvand, M., Ahmadi, M., Shadizadeh, et al. (2013). Geological storage of carbon dioxide by injection of carbonated water in an Iranian oil reservoir: A case study. *Journal of Petroleum Science and Engineering , 111*, 170-177.

Haugan, P., Drange, H. (1996). Effects of CO_2 on the ocean environment. *Energy Convers, 37*(6-8), 1019-1022.

Herzog, H. (1998). Ocean sequestration of CO_2 - An overview.

Herzog, H., Vukmirovic, N. (n.d.). CO_2 sequestration: opportunities and challenges.

IEA Greenhouse Gas R&D Programe (2000). Capture of CO_2 using water scrubbing.

IPCC. (2013). Fifth Assessment Report of the Intergoernmental Panel on Climate Change.

Kaufmann, G., Dreybrodt, W. (2007). Calcite dissolution kinetics in the system $CaCO_3$-H_2O-CO_2 at high undersaturation. *Geochimica et Cosmochimica, 71*, 1398-1410.

Kirchner, J. S., Lettmann , K., Shnetger , B., et al. (2020). Carbon capture via accelerated weathering of limestone: Modelling local impacts on the carbonate chemistry of the southern North Sea. *International Journal of Greenhouse Gas Control, 92*.

Kirchner, J., Berry, A., Ohnemuller, F., et al. (2020). Reducing CO_2 Emissions of a Coal-Fired Power Plant via Accelerated Weathering of Limestone: Carbon Capture Efficiency and Environmental Safety. *Environmental Science & Technology*.

Koenen, M., Neele, F., Van der Valk, K., Kervèvan, C. (2019). Techno-economic impact of CO_2 co-injection into geothermal doublets for the Netherlands. *European Geothermal Congress* .

Lea, A., Amonette, J., Baer, et al. (2001). Microscopic effects of carbonate, manganese, and strontium ions on calcite dissolution. *Geochimica et Cosmochimica, 65*(3), 369-379.

Lyman , J., Fleming, R. (1940). Composition of sea water. *Journal of Marine Research*.

Matter, J., Stute, M., Snaebjornsdottir, S., et al. (2016). Rapid carbon mineralization for permanent disposal of anthropogenic carbon dioxide emissions. *Research, 352*, 1312-1314.

Middelburg, J., Soetaert, K., Hagens, M. (2020). Ocean Alkalinity, Buffering and Giogeochemical Process. *Reviews of Geophysics*, 1-28.

Mucci, A., Morse, J. (1983). The incorporation of Mg^{2+} and Sr^{2+} into calcite overgrowths: influences of growth rate and solution composition. *Geochimica et Cosmochimica, 47*, 217-233.

Naviaux, J., Subhas, A., Dong, S., et al. (2019). Calcite dissolution rates in seawater: Lab vs in-situ measurements and inhibition by organic matter. *Marine Chemistry, 215*.

Rau , G., Caldeira, K. (1999). Enhanced carbonate dissolution: a means of sequestering waste CO_2 as ocean bicarbonate. *Energy COnversion & Managment, 40*, 1803-1813.

Rau, G. (2010). CO_2 Mitigation via Capture and Chemical Conversion in Seawater. *Environmental Science & Technology*.

Rau, G., Caldeira, K. (2004). *US Patent No. Us 7,655,193 B1*.

Rau, G., Caldeira, K., Knauss, et al. (2001). *Enhanced carbonate dissolution as a means of capturin and sequestering carbon dioxide.*

Rau, G., Knauss, K., Langer, W., Caldeira , K. (2007). Reducing energy-related CO_2 emissions using accelerated weatering of limestone. *Energy, 32*, 1471-1477.

Renforth, P., Henderson, G. (2017). Assessing ocean alkalinity for carbon sequestration. *AGU Reviews of Geophysics*.

Scripps Institute of Oceanography. (2020). Retrieved from https://scripps.ucsd.edu

Shariatipour, S., Mackay, E., Pickup, G. (2016). An engineering solution for CO_2 injection in saline aquifers. *International Journal of Greenhouse Gas Control, 53*, 98-105.

Sigfusson , B., Gislason, S., Matter, J., et al. (2015). Solving the carbon-dioxide buoyancy challenge: THe design and field testing of dissolved CO_2 injection system. *International Journal of Greenhouse Gas Control, 37*, 213-219.

Strogen, D., Arnot, M., Bland, K., & Griffin, A. (2009). Opportunities for underground geological storage of CO2 in New Zeland. *GNS Science Report*, 104.

Subhas, A., Rollins, N., Berelson, et al. (2015). A novel determination of calcite dissolution kinetics in seawater. *Geochimica et Cosmochimica, 170*, 51-68.

Tannenberg, M. (2009). *Settling and Dissolution of Calcium Hydroxyde Particles.*

Torp, T., Gale , J. (2004). Demonstrating storage of CO_2 in geological reservoirs: The Sleipner and SACS projects. *Energy, 29*, 1361-1269.

UNFCC. (2015). *Paris Agreement.*

USGS science for a changing world. (2020, 9 5). Retrieved from https://www.usgs.gov

van der Spek, M., Fout, T., Garcia, M., et al. (2020). Uncertainty analysis in the techno-economic assessment of CO_2 capture and storage techologies. Critical reveiw and guidelines for use. *International Journal of Greenhouse Gas Control, 100*.

Xu, M., Higgins, S. (2011). Effects of magnesium ions on near-equilibrium calcite dissolution: Step kinetics and morphology. *Geochimica et Cosmochimica, 75*, 719-733.